Energy, Mines and Resources Canada

Énergie, Mines et Ressources Canada

CANMET

Canada Centre for Mineral and Energy Technology

Centre canadien de la technologie des minéraux et de l'énergie

Mining Research Laboratories

Laboratoires de recherche minière

Canada

91-06269/

RADIOACTIVE DUST SAMPLING
PART 1: LABORATORY TEST FACILITIES USED AND SAMPLING INSTRUMENTATION EVALUATED

J. Bigu and A. Frattini

DIVISION REPORT MRL 91-074 (TR) MAY 1990

This document is an unedited internal report prepared primarily for discussion and retrieval purposes. It does not represent a final expression of the opinion of the Canada Centre for Mineral and Energy Technology (CANMET)

Ce document est un rapport provisoire non-révisé et rédigé principalement pour fin de diffusion et de documentation au sein du Centre canadien de la technologie des minéraux et de l'énergie (CANMET)

72 pp

MICROMEDIA

MICROMEDIA

RADIOACTIVE DUST SAMPLING
PART I - LABORATORY TEST FACILITIES USED AND SAMPLING INSTRUMENTATION EVALUATED

J. Bigu* and A. Frattini**

ABSTRACT

This technical report is part of a series of reports on the technical evaluation of several dust monitoring instruments in common use in specialized laboratory and field work. The first part of the series (the present work), describes the instrumentation which was evaluated under laboratory-controlled conditions, as well as in an underground uranium mine in Ontario, and two uranium mills in Saskatchewan. The report also describes and discusses the laboratory test facility used for the laboratory evaluation of the instrumentation. This special facility, known as the Long-Lived Radioactive Dust Test Facility (LLRDTF), was designed for the simulation of radioactive aerosol atmospheres, for radioactive atmosphere modelling purposes, and for the testing and calibration of radioactive dust monitoring devices.

Key words: Radioactive dust; Radiation sampling; Dust characterization.

*Research Scientist, **Technologist, Elliot Lake Laboratory, CANMET, Energy, Mines and Resources Canada, Elliot Lake, Ontario.

PRÉLÈVEMENT DE POUSSIÈRES RADIOACTIVES PARTIE I - ÉVALUATION DES INSTALLATIONS D'ESSAI ET DES APPAREILS DE PRÉLÈVEMENT

J. Bigu* et A. Frattini**

RÉSUMÉ

Le présent rapport technique fait partie d'une série de rapports sur l'évaluation technique de plusieurs détecteurs de poussières, qui sont utilisés fréquemment au cours de travaux spécialisés menés en laboratoire et sur le terrain. La première partie de la série (l'ouvrage actuel) décrit les appareils qui ont été évalués en laboratoire dans un milieu conditionné, dans une mine souterraine d'uranium en Ontario et dans deux usines de traitement de l'uranium en Saskatchewan. Les auteurs présentent une description et une discussion de l'installation d'essai utilisée pour évaluer des appareils. Cette installation spéciale, connue sous le nom d'Installation d'essai des poussières radioactives de longue période (IEPRLP), a été conçue aux fins de la simulation des atmosphères d'aérosols radioactifs, de la modélisation des atmosphères radioactives, de la mise à l'essai et de l'étalonnage des détecteurs de poussières radioactives.

Mots clés : poussière radioactive; échantillonnage de la radiation; caractérisation des poussières.

*Chercheur scientifique et **technologue, Laboratoire de Elliot Lake, CANMET, Énergie, Mines et Ressources Canada, Elliot Lake (Ontario)

CONTENTS

	Page
ABSTRACT	i
RESUME	ii
INTRODUCTION	1
SCOPE OF EXPERIMENTAL WORK	3
THE LONG-LIVED RADIOACTIVE DUST TEST FACILITY (LLRDTF)	6
1. Theoretical Background	10
2. Experimental Evaluation of the LLRDTF	12
INSTRUMENTATION USED - INTRODUCTION	14
DESCRIPTION OF INSTRUMENTATION	16
Cascade Impactors	16
Cyclones	25
The Open-Face Filter Sampler	27
(PAD) The Personal α-Particle Dosimeter	27
Optical Particle Counters	29
REFERENCES	33

FIGURES

No.		
1.	Simplified view of the Long-Lived Radioactive Dust Test Facility (LLRDTF)	36
2.	Front view of the LLRDTF showing windows, doors, sampling ports and other components	37
3.	Rear view of the LLRDTF showing windows, doors, samplilng ports and other components	38
4.	Top view of the LLRDTF showing windows, sampling ports, valves, and other components	39
5.	Air velocity versus width in section A (S.A) of the LLRDTF for a fixed height (10.2 cm) and distance (0 cm) from the opening of S.A.	40
6.	Air velocity versus width in Section A (S.A) of the LLRDTF for a fixed height (30.5 cm) and distance (61 cm) from the opening of S.A	41
7.	Air velocity versus width in section A (S.A) of the LLRDTF for a fixed height (45.7 cm) and distance (61 cm) from the opening of S.A	42
8.	Air velocity versus width in section A (S.A) of the LLRDTF for a fixed height (10.2 cm) and distance (244 cm) from the opening of S.A	43
9.	Air velocity versus distance from the opening of section A (S.A) for a fixed height (10.2 cm) and width (40.6 cm) of S.A	44

10. Air velocity versus distance from the opening of section A (S.A) for a fixed height (30.5 cm) and width (81 cm) of S.A 45

11. Air velocity versus width in section B (S.B) of the LLRDTF for a fixed height (33 cm) and distance (15 cm) from the opening of S.B . 46

12. Air velocity versus distance from the opening of section B (S.B) for a fixed height (15.2 cm) and width (15.2 cm) of S.B 47

13. Air velocity versus distance from the opening of section B (S.B) for a fixed height (33 cm) and width (76 cm) of S.B 48

14. Air velocity versus width in section C (S.C) of the LLRDTF for a fixed height (10.2 cm) and distance (46 cm) from the opening of S.C. 49

15. Air velocity versus width in section C (S.C) of the LLRDTF for a fixed height (20.3 cm) and distance (76 cm) from the opening of S.C 50

16. Air velocity versus distance from the opening of section C (S.C) for a fixed height (10.2 cm) and width (51 cm) of S.C 51

17. Air velocity versus distance from the opening of section C (S.C) for a fixed height (20.3 cm) and width (51 cm) of S.C 52

18. View of cascade impactor Sierra 210 53

19. View of the cascade impactor Marple 290 with sampling pump (left hand side) and without the pump (right hand side) 54

20. PC-2 aerosol analyzer 55

21. Flow diagram of PC-2 with PC-202 high concentration sliding valve . 56

22. Details of the crystal assembly (upper drawing, and crystal (lower drawing) 57

23. Nylon cyclone 58

24. General view of an open-face dust sampler 59

25. Views of the CEA track etch dosimeter (PAD) 60

26. View of the CEA track etch dosimeter and components 61

27. Details of CEA track etch dosimeter sampling head 62

28. Main view of MiniRam 63

29 a) Zero check module 64

b) MiniRam with zero check module attached 64

c) MiniRam with flow adapter attached 64

d) Flow adapter 64

30 a) Personal sampler adapters 65

b) MiniRam with personal sampler adapter attached 65

c) Respirator adapter 65

d) MiniRam with respirator adapter attached 65

31. Front view of the OPC CI-7300 (left hand side) and control panel of the same instrument (right hand side) 66

32. Air sampling system (left hand side), and optical system (right hand side) of the OPC CI-7300 67

INTRODUCTION

Mining and milling operations generate dust emissions within a wide particle size range - from submicron size to well beyond the respirable size range. Of particular interest from the occupational hygiene and health physics viewpoints are dusts in the respirable particle size range, namely, from less than 1 μm (~0.3 μm) to approximately 10 μm. Dust in this particle size range, once inhaled, will be deposited in different parts of the respiratory system in amounts which depend on some characteristics of the dust such as particle size distribution and electrical charge (1-10).

In uranium mining, processing and refining industries, dust emissions contain a variety of radionuclides (2-6,11). The inhalation of these dusts poses a serious occupational health hazard to industrial workers (12,13). Dusts generated in uranium industrial operations contain the parents of the natural uranium and thorium radioactive decay chains (^{238}U, ^{235}U, and ^{232}Th), as well as their long-lived decay products (^{226}Ra, ^{228}Th, ^{230}Th, ^{234}U, and others) and short-lived decay products (^{222}Rn progeny and ^{220}Rn progeny). Dusts that contain long-lived radionuclides are commonly referred to as Long-Lived Radioactive Dust (LLRD). However, because of the decay of these long-lived radionuclides into short-lived radioisotopes, short-lived radioactivity is also associated with LLRD. The most hazardous type of radiation associated with LLRD is α-particle emission (particles) whose energy is totally absorbed in about 100 μm of tissue.

Because of the potential occupational health hazards associated with the inhalation of LLRD, its characterization is of great practical importance. Sampling and monitoring instrumentation, methods and techniques for the characterization of dust, and of its associated radioactivity, are relevant items in the calculation of occupational radiation exposures of industrial workers, and in ascertaining that LLRD control methods operate efficiently.

Accurate characterization of Long-Lived Radioactive Dust (LLRD), e.g.,

concentration, size distribution, radioisotope make-up and chemical composition, permits the calculation of the Committed Effective Dose Equivalent (H_{50}) (12-14), an important biophysical quantity. Knowledge of H_{50} allows estimation of the workers' internal radiation exposure by means of standard internal dosimetry methods (12-14).

It is quite evident that the reliable and accurate characterization of LLRD is of crucial importance for the evaluation of the occupational radiation health hazards to which occupational (industrial) workers are exposed. Accurate LLRD characterization depends, in turn, on reliable instrumentation, as well as in the strict adherence to certain sampling and monitoring protocols, methods and techniques.

There is a disturbing lack of information regarding the accuracy, performance, and behaviour of LLRD sampling methods, techniques and monitoring instrumentation. In particular, there is a significant gap with regard to direct performance comparisons of different types of instruments commonly used in the characterization of dust clouds. In a previous report, the author reviewed several topics related to this subject (15). In this report, extensive experimental data are presented on the performance of a number of dust sampling instruments in common routine field use, as well as of other instrumentation in more restrictive and delicate applications for research or other purposes.

The work presented here was conducted in a dust test facility especially designed for this type of work and known as the Long-Lived Radioactive Dust Test Facility (LLRDTF), as well as under field conditions in an underground uranium (U) mine and two uranium mills. This work was requested by the Atomic Energy Control Board (AECB) as part of a contract awarded to CANMET (EMR), entitled "Comparison of Radioactive Aerosol Sampling Instruments", AECB Contract No. 4.108.1; Mining Research Laboratories (CANMET) Project No. 143902-14-4. Phase I of this contract was completed (and

a report was submitted to the AECB, March 1990) under the title "A Review of Airborne Particle Sampling with Special Reference to Long-Lived Radioactive Dust".

SCOPE OF EXPERIMENTAL WORK

The scope of the work presented here is twofold:

1. Characterization of radioactive dust (LLRD) at conventional working locations typical of mechanical and physico-chemical operations related to the mining, extraction, processing and refining of uranium (U) ores;
2. Evaluation of the performance of a number of different instruments designed for the sampling, monitoring and characterization of dust.

Item 1) is important from the occupational hygiene standpoint. Information on dust (e.g., particle size distribution and radioisotope make-up), in conjunction with the use of theoretical models of the respiratory system, is relevant for internal dosimetry calculation purposes. This, in turn, greatly facilitates the evaluation of the potential health risks associated with the inhalation of LLRD by industrial workers in the U industry, and other related industries.

Item 2) is relevant in an entirely different context. Owing to large differences in the characteristics of industrial dusts (e.g., particle size distribution, electrical charge distribution, chemical composition, toxicity, radioisotope make-up, and specific radioactivity), the performance and behaviour of different dust monitoring and sampling instruments exposed to the same dust cloud may significantly differ from each other. This, in turn, will affect the accuracy of dust characterization, and hence, the estimation of health hazards of workers exposed to industrial dusts.

Items 1) and 2) have been amply covered in the work conducted by the Elliot Lake Laboratory (ELL, MRL, CANMET) personnel. Thus, data (dust characterization) have been gathered at different working locations, namely,

an underground U-mine in Elliot Lake, and two U-mills in Saskatchewan. Furthermore, a considerable amount of data has been collected under laboratory-controlled conditions using a Long-Lived Radioactive Dust Test Facility (LLRDTF) designed for this purpose.

With regards to the field work at the U-mine and U-mills, the dust characterization and the performance evaluation of the instrumentation used were, understandably, carried out under 'natural' field conditions, i.e., using the 'undisturbed' (by the researchers) LLRD generated in the various mining and milling operations monitored.

The work conducted under laboratory-controlled conditions in the LLRDTF was carried out using several kinds of 'non-radioactive' and 'radioactive' dusts. Talcum powder, flour, Al_2O_3 and SiC are included in the first category. Finely ground and milled uranium tailing powders fall in the second category. The characteristics of the above dusts will be discussed and described in another report. The variables measured in these dusts, as well as in the industrial dusts (U-mine and U-mills) were as follows:

1. Particle size distribution;
2. Radioactive size distribution;
3. From items 1) and 2), the Mass Median Aerodynamic Diameter (MMAD), and the Activity Median Aerodynamic Diameter (AMAD), respectively, were calculated as well as their corresponding geometric standard deviations, denoted by σ_g;
4. Particle and mass concentration;
5. Radioactivity associated with the dust, i.e., activity concentration, denoted by [LLRD];
6. Specific activity, SA, representing the (α-particle) radioactivity per unit mass of dust;
7. In a number of cases, the electrical charge distribution was measured.

Instrumentation of a diverse nature was evaluated in these studies.

These comprised instruments operating on different physical principles, as well as in discrete (grab-sampling) and 'continuous' fashion. The characteristics of these instruments will be described below.

Because of the volume of data collected, as well as for the sake of simplicity, the present work will be presented in several parts, i.e., reports.

The reader should be cautioned that the instruments tested in this work, and with which all the data presented here were obtained, were operated according to the instructions, recommendations and analytical procedures supplied by their respective manufacturers in their instruction manuals. Hence, no attempt has been made at any phase of this work to verify by independent means, i.e., calibration procedures, the accuracy of the claims made by the manufacturers regarding the technical performance of their instruments. This would have entailed work beyond the scope of this contract, such as the measurement of the collection efficiency of the impactor stages of the cascade impactors used, and the determination of the counting efficiency of the optical particle counters tested. In both cases, thorough and time-consuming measurements would have been needed requiring extensive use of highly monodisperse aerosol sources of a diverse type, e.g., particle size and chemical composition.

As a result of the above, the evaluation of the instrumentation carried out here will not help, in a number of cases, to decide which instrument(s) perform best under a given set of experimental conditions. Rather, the most important conclusion to be drawn from this work, and indeed one of tantamount practical importance, is the empirical fact that different instruments exposed to identical dust conditions give significantly different dust characterizations. Owing to a variety of reasons, different individuals or companies use different instruments to measure airborne pollutants such as radioactive dust, or simply dust, for air quality control purposes, and to

report data to the pertinent regulatory agencies for compliance purposes. Because these data are then used to estimate the occupational exposure of industrial workers, the importance of the accuracy of the experimental data cannot be sufficiently emphasized, since it will reflect directly on the health of the workers.

It should be noted that dust characterization, as measured by different instruments, falls into two main categories, namely:

a) total particle concentration, and particle number versus particle size distribution;

b) mass concentration, and particle mass versus particle size distribution.

It will be left to the interested reader to differentiate some of the subtleties and idiosyncrasies characteristic of each instrument as well as to decide on their implications from an engineering, regulatory, and health physics standpoints.

As previously indicated, the second, and final, phase of the project "Comparison of Radioactive Aerosol Sampling Instruments" will be presented in several reports. The first report (present report) will present a detailed description of the instruments used in this project, as well as a brief description and discussion on the characteristics and performance of the Long-Lived Radioactive Dust Test Facility (LLRDTF), i.e., the test facility used for laboratory experimentation. The second report will deal with the experimental work conducted in the LLRDTF. The third report will present and discuss the experimental data obtained at an underground (UG) uranium (U) mine. The fourth report will deal with the work conducted at two U-mills. Finally, the fifth report will present an overall or 'global' discussion of all the data obtained in the field and in the laboratory.

THE LONG-LIVED RADIOACTIVE DUST TEST FACILITY (LLRDTF)

The Long-Lived Radioactive Dust Test Facility (LLRDTF) was designed

with a four-fold purpose in mind, namely:

a) To generate and simulate radioactive dust atmospheres either approaching idealized, custom-made conditions, or representing actual field conditions in underground and open pit uranium mines, uranium mills and other radioactive dust environments;

b) To characterize Long-Lived Radioactive Dust (LLRD), i.e., particle size and particle mass distributions, particle electrical charge distribution, particle number and mass concentration, etc.;

c) To verify and model radioactive aerosol environments;

d) To evaluate, test and calibrate instrumentation used for the characterization and quantification of LLRD.

The design of the LLRDTF was slightly affected by space considerations and practical constraints. However, these limitations did not unduly affect the overall performance of the test facility because the LLRDTF was intended for operation in the turbulent and sub-turbulent, i.e., transition, airflow regimes rather than under laminar flow conditions.

The LLRDTF consists of three main body sections (referred to as A, B and C), or test areas, of different physical dimensions for the purpose of conducting simultaneous tests, simulations or dust characterizations in three different locations of the installation under different airflow conditions (see Figure 1). The external dimensions of the three sections (L x H x W), where L, H, W stand, respectively, for length, height and width, are as follows:

Section A: 2.44 m x 1.21 m x 1.31 m

Section B: 1.22 m x 0.56 m x 1.02 m

Section C: 0.92 m x 0.41 m x 0.71 m.

The effective test volumes for sections A, B and C are approximately 3.7 m^3, 0.6 m^3, and 0.25 m^3, and their respective cross-sectional areas are 1.6 m^2, 0.6 m^2, and 0.3 m^2. Because of airflow conservation, and neglecting

friction losses, the above dimensions indicate that the ratios of air velocities between sections A and C and sections A and B are about 5 and 2.5, respectively. (These figures can be easily calculated from the mass conservation laws, namely: $v_A S_A = v_B S_B = v_C S_C$ where, v and S are, respectively, the air velocity and cross-sectional area of the section under consideration, and the sub-indices A, B and C refer to the testing sections indicated above.)

The LLRDTF can operate in a recirculation mode and in a flowthrough, single-air-pass fashion. These options are effected by means of three main valves of the butterfly type in the airflow system in conjunction with a fan of the centrifugal kind providing an airflow rate in the LLRDTF which can be varied with relative ease. The three test sections A, B and C, and the fan are linked to the rest of the facility by means of couplings that provide a smooth transition between cross-sections of different surface areas, and 90° 'bends' made of circular tubing.

The LLRDTF has an overall length of slightly more than 6 m and is shaped in a closed, elongated loop configuration that meets the important requirements of maximum and optimum performance in a minimum of space (see Figures 1 to 4).

This dust test facility is equipped with a number of removable and fixed windows and doors for a threefold purpose:

a) to position or locate, access, and retrieve instrumentation and other objects or items placed inside the LLRDTF;
b) to view objects and read instrumentation placed inside the test facility; and
c) to allow light from the laboratory space to illuminate the inside of the LLRDTF.

The following windows and doors are available for the above purposes (see Figures 2 to 4):

Section A: 2 medium-size doors, 1 large door, and 2 small removable windows;

Section B: 1 medium size removable window;

Section C: 1 medium size removable window.

Furthermore, windows were installed on the side and top of the transitions leading to Section A from the airflow system of the LLRDTF (left hand side of section A in Figures 2 and 4), and from section A to the fan. The windows installed on the side of the transitions are removable for maintenance purposes, whereas those located on the top of the transitions are fixed, i.e., cannot be opened.

A special mechanical design permits easy opening of the doors with minimum effort. A special feature of the mechanism used in the doors is that the latter will remain open at any position desired. Doors and windows are constructed of a solid frame where thick glass panels, ~6 mm thickness, are fitted leak-free. The body of the LLRDTF is fitted with special built-in gaskets that ensure excellent air-tight conditions when the doors are closed and the windows are in position.

The joints of the LLRDTF were sealed with a silicone sealant and the joints and the inside walls of the installation (after priming) were treated with several coatings of an epoxy resin-based paint of undisclosed formulation to reduce the diffusion of gases to a minimum outside the volume of the LLRDTF.

The radioactive dust test facility is equipped with a number of sampling and injection ports in order to make it possible to:

a) inject dusts and radioactive gases;

b) take air samples; and

c) monitor airflow conditions.

Special stainless steel valves and fittings are provided in the walls of the LLRDTF to carry out items a) to c). A special feature of this test facility is that provisions exist to inject radioactive gases such as radon

(^{222}Rn) and thoron (^{220}Rn) to neutralize and/or charge LLRD, among several other features that will be discussed in a forthcoming report.

Although the LLRDTF was primarily designed to operate at normal ambient conditions of temperature, T, and relative humidity, RH, these conditions can be varied within a reasonably wide range for special applications. Furthermore, ion-concentration in the test facility can also be varied at will by special instrumentation designed for the purpose.

A detailed account of the airflow characteristics and performance of the LLRDTF is beyond the scope of this report. However, the latter would not be complete without a minimum of documentation necessary to help in understanding and interpreting the data which are presented in subsequent sections or reports.

The rest of this section will be devoted to the presentation of some practical expressions for the readers' benefit in the hope that they may be helpful in assessing the performance of the installation in relation to the experimental work carried out in it. This brief presentation will be followed by some airflow characterization data for the LLRDTF.

1. THEORETICAL BACKGROUND

A very important variable in airflow characterization is the Reynolds number, Re, which can be thought of as an index of turbulence, and which is defined by:

$$Re = \rho L \upsilon / \mu \qquad \text{Eq 1}$$

where, ρ is the air density,

L is a characteristic dimension, e.g., length of the system,

υ is the air velocity,

μ is the air viscosity.

Turbulent flow occurs for Re $\gtrsim$ 2200.

For circular ducts the characteristic dimension is the diameter of the duct. However, for non-circular ducts L should be replaced by the so-called

hydraulic mean diameter, say L_h, which is given by: $L_h = 4S/P$. In this expression S is the cross-sectional area of the duct, and P is its perimeter. It is clear that for a square duct $S = L^2$, and $P = 4\ L$. Hence, $L_h = L$.

Another variable useful in the design of installations such as the LLRDTF and in the testing and evaluation of ducts,transitions, couplings and the like is the (dynamic) frictional loss which manifests itself as a pressure loss, ΔP_D, given by:

$$\Delta P_D = (\rho v^2/2)(fl/d) \qquad \text{Eq 2}$$

where, f is the friction factor,

l is the length of the duct, pipe, etc., and

d is the diameter of the duct, pipe, etc.

The friction factor, f, depends on the surface condition (roughness) of the walls of the duct, pipe, etc. and on the Reynolds number. The friction factor f increases with increasing air velocity and surface roughness.

The first term in round brackets in the above expression represents a velocity loss, i.e., velocity pressure loss (ΔP_v), whereas the second term in brackets represents a purely geometrical factor, F_G, which depends on the geometry of the section, i.e., physical dimensions, and on the physico-geometrical or morphological characteristics of the surface or wall under consideration, e.g., roughness. Hence, we may write:

$$\Delta P_D = \Delta P_v F_G \qquad \text{Eq 3}$$

Static pressure losses, ΔP_s, are estimated in the usual way by means of:

$$\Delta P_s = \rho g H \qquad \text{Eq 4}$$

where, H is height relative to a reference level, or alternatively, to the elevation change.

The calculations for ΔP_D, Re, and other useful variables for the LLRDTF facility are the subject of a forthcoming report. In the remainder of this section, i.e., next sub-section, airflow characterization of the LLRDTF will

be presented and discussed.

2. EXPERIMENTAL EVALUATION OF THE LLRDTF

Of particular relevance in the performance evaluation of the LLRDTF are the airflow characteristics of the test facility, e.g., the airflow rate spatial distribution in sections A, B and C, and other areas of potential interest in the installation. Variables of interest are the airflow rate, Q, and the air velocity, v, which are related by the simple relationship $Q = vS$. The airflow rate is a function of the characteristic of the fan, e.g., fan blade shape and surface area, speed of the fan (rpm), and the like. For a given set of the above parameters, and because of mass conservation considerations, Q remains the same, independent of the cross-sectional area through which the mass of air flows. The above is only true if there are no air leaks in the system and friction losses are ignored. For a given mass airflow, the air velocity varies inversely with the cross-sectional area, i.e., $v = KS^{-1}$, where K is a constant, in this case Q.

Both Q and v are key variables in the simulation of LLRD atmospheres and in the performance evaluation of radioactive dust monitoring instrumentation. In the context of our study, namely, the evaluation of radioactive aerosol instrumentation, it is important for the instruments tested to sample air under the same airflow conditions, i.e., same air velocity, v, as well as under isokinetic conditions.

A practical difficulty that deserves special attention, and which arises frequently in the concurrent evaluation of closely spaced instruments is that of mutual interference and self-interference. In order to avoid these effects, the instruments to be tested should be sufficiently far from one another to minimize or altogether avoid:

a) LLRD shielding effects;

b) undesirable airflow patterns about the instrumentation; and

c) sampling conditions in one instrument affecting conditions in another

instrument.

Meeting the requirements necessary to avoid the practical difficulties outlined in items a) to c) not only necessitates a relatively large volume, but also fairly constant airflow conditions, i.e., air velocity, over this volume. In summary, airflow conditions over the LLRDTF testing section (volume) should be as uniform as practically possible.

Airflow rate (and cross-sectional area) measurements in the LLRDTF were conducted for several fan settings, i.e., fan speed (rpm) in order to fully characterize the installation and to select a suitable section of the test facility to carry out the evaluation of the instrumentation which is the main subject of this study. However, the data presented here are limited to one fan speed only, i.e., an arbitrarily fixed value of Q suitable for the purpose of this investigation. Data for other values of Q, i.e., other fan speeds, will be presented in another report.

Airflow measurements, e.g., air velocity, were conducted using air velocity probes in conjunction with their associated data acquisition systems (DAS) and by conventional Pitot tubes in conjunction with differential manometers and Magnehelics. The air velocity probes and DAS used were manufactured by Thermal Systems Incorporated (T.S.I., U.S.A.). Models 1610-4 and 1620, for air velocity probes, and a DAS (Linear Signal Conditioner) model 67, were used in the measurements.

Some of the data obtained are shown in Figures 5 to 17. Measurements were carried out in Sections A, B and C. Several cross-sections for each section (i.e., A, B, C) were chosen and the air velocity for each cross-section was mapped in the plane perpendicular to the airflow. In addition, the air velocity was measured along planes perpendicular to the floor of each section, i.e., planes parallel to the direction of the airflow. In Figures 5 to 17, the height is measured from the floor of each section as the reference plane. The distance of the plane perpendicular to the direction of the

airflow where measurements are conducted is indicated by the variable x. (Note: x is taken as the distance from the plane which joins the section under consideration and its corresponding duct transition. This variable is the same as the y-axis labelled Distance (length) in some graphs.) The variable y refers to the distance measured from the walls of the section under consideration perpendicular to the floor of the section and parallel to the direction of the flow of air. This variable is the same as the x-axis labelled Distance (width) in some graphs.

Figures 5 to 10 show air velocity data for section A. Figures 11 to 13, and Figures 14 to 17 show air velocity data for sections B and C, respectively. From the data in these figures and for the specific fan setting in these series of measurements, Figures 5 to 17 show that an air velocity range of less than 0.5 m/s to more than 4.5 m/s can be attained without difficulty. Higher (lower) fan settings permit higher (lower) air velocity ranges to be attained. The LLRDTF was normally operated at an airflow rate of about 2 m^3/s. It is not difficult to calculate the Reynolds number (Re) using Equation 1 and the values for the air velocity given above. For section A, where the majority of the tests were conducted, Re can be calculated by taking into account that for air at NTP $\rho = 1.2$ kg/m^3, and $\mu = 1.8 \times 10^{-5}$ Ns/m^2. Taking L = 1.2 m and $v = 1$ m/s:

$$Re = 1.2 \times 1.2 \times 1.0/(1.8 \times 10^{-5}) = 0.8 \times 10^5$$

The instruments to be evaluated were located in section A in the LLRDTF. They were confined to a volume over which the air velocity profile remained essentially constant and 'shadow' and interference effects were thought to be kept to a minimum.

INSTRUMENTATION USED - INTRODUCTION

A number of instruments operating on different principles were evaluated and compared. The instrumentation tested fell into two main

categories, namely, grab-sampling devices and continuous monitoring devices. A further classification based on the physical principle of operation is both useful and convenient. Again two major categories are of practical interest in the context of this work:

1. Inertial and gravitational dust devices; and
2. Optical particle counters (OPC).

The instruments tested in this experimental project are listed below:

1. Cascade impactors;
2. Nylon cyclones;
3. Open face dust collectors;
4. Personal α-particle dosimeters (PAD); and
5. Optical particle counters.

Three different types of cascade impactors were used, two of the 'mechanical-manual' type, and one fully automated cascade impactor of the 'electronic' type. The mechanical-type cascade impactors will be referred to hereafter as Sierra-210 and Marple-290. The 'electronic' cascade impactor will be referred to hereafter as the QCM.

The acronym PAD refers here to an α-particle personal dosimeter, which uses track-etch detection techniques, developed by the Commissariat à la Energie Atomique (CEA) of France. This device was designed for personal dosimetry of radon (^{222}Rn) and thoron (^{220}Rn) progeny. In our case, the dosimeter is used for collecting and quantifying airborne radioactive dust.

Two different types of optical particle counters were used, namely, Model CI-7300 manufactured by CLIMET Instruments (U.S.A.), and MiniRam Model PDM-3 manufactured by CGA (U.S.A.). There is a significant difference between these two optical instruments as will be discussed below.

A classification of the instruments tested according to the definitions given earlier is given below:

Instrument	Classification
Sierra 210	GS, IGDD, manual
Marple 290	GS, IGDD, manual
QCM	GS, IGDD, automated
Nylon cyclone (NC)	GS, IGDD, manual
Open face dust collector (OF)	GS, IGDD, manual
PAD	GS, manual
Climet CI-7300	OPC, CM, automated
MiniRam PDM-3	OPC, CM, automated

where, in the above list the meaning of the abbreviations given is as follows:

GS stands for grab-sampling device;

CM stands for continuous monitoring device;

OPC stands for optical particle counter;

IGDD stands for inertial and gravitational dust device.

Furthermore, the abbreviations NC and OF stand, respectively, for nylon cyclone and dust collector of the open face type.

The next section is devoted to a detailed description of the instruments tested, evaluated and compared in the course of the experimental work pertaining to phase II of the present AECB contract. Additional information can be found in the report "Comparison of Radioactive Aerosol Sampling Instruments", phase I (15).

DESCRIPTION OF INSTRUMENTATION

This section deals with discussion and description of the characteristics of the different instruments evaluated. Cascade impactors and other inertial-gravitational dust collecting devices will be described first followed by optical particle counters. Open face collecting devices and the PAD will be included in the first category.

CASCADE IMPACTORS

Devices that remove airborne particles through mechanical impaction

processes, i.e., particle deposition occurring when airflow streamlines bend sharply as the airflow bypasses a solid object, are known as impactors. The name cascade impactor refers to the case where a number of single stage impactors are stacked together in series, each stage impactor having different particle cut-size characteristics. A description of the two types of cascade impactors used in this study, namely, the Sierra 210 and the Marple 290 follows.

A. Cascade Impactor Sierra 210

The Sierra 210 is a multi-stage cascade impactor which can accommodate up to 10 impactor stages covering a particle size cut-off range, at 50% collection efficiency ($D_{p,50}$), from nominally 0.05 μm to 20 μm. The impactor stages have a radial (rectangular) slot design consisting of four slots in a right angle cross-shape configuration. The stages are labelled No. 1 (first stage) to No. 10 (last stage) following the direction of the airflow in the device. The first stage (No. 1) is designed to remove the largest dust particle size; subsequent ever increasing stage numbers are designed to remove ever decreasing particle sizes. The width of the slots corresponding to each impactor stage varies according to the stage number decreasing with increasing cascade impactor stage number. Dust particles not collected in, that is, escaping the last stage number are deposited in a 'back-up' glass fibre filter.

The radial slot impactor design of the Sierra 210 creates a circumferential airflow between stages, resulting in very low inter-stage, i.e., wall, particle losses. Dust particles entering the cascade impactor are collected on substrates sitting on each stage and matching the four slot designs exactly. Substrate materials are in a majority of cases glass fibre or stainless steel. In our case, glass fibre substrates have been used.

The Sierra 210 can be operated with any number of stages between 4 and 10, although for most cases it is best to use 8 to 10 stages. Eight stages

were used in all the data reported in this study. One serious problem with cascade impactor usage is dust loading caused by sampling for too long for a given dust concentration, C. Excessive sampling causes certain stages to become overloaded and particle re-entrainment may occur. Sampling for too short a period may result, however, in too little mass on some stages for accurate weighing. The minimum loading should be in the range 0.2 to 0.5 mg. The maximum loading depends on the type and wetness of the dust particles. For dry particles, the loading should not exceed 1 to 2 mg. Higher loadings are possible if the particles are liquid or wet.

The average loading, W (mg), per stage can be calculated with the following expression:

$$W = 10^{-3} CQt/n \qquad \text{Eq 5}$$

where, Q is the sampling flow rate, L/min

t is the sampling time, min

n is the number of impactor stages plus the filter stage, i.e., back-up filter, and the cyclone stage (see below).

The Sierra 210 is equipped with a cyclone preseparator to remove dust particles larger than the largest particle sizes that can be removed by the first stage of the cascade impactor. The theory of cyclones has been examined elsewhere (15), and will be briefly examined again below. Of interest is the cut-point, D_p, of the cyclone given by the following expression:

$$D_p = k\eta/Q\rho_p{}^{1/2} \qquad \text{Eq 6}$$

where, K is a constant

η is the gas viscosity (g/cm s)

ρ_p is the particle mass density (g/cm^3)

A variable of great practical value is the particle size cut-off at 50% collection efficiency for spherical particles, namely, $D_{p,50}$. This variable can be calculated by:

$$D_{p,50} = w\ St^{1/2}(9\eta L/C\rho_p Q)^{1/2} \qquad \text{Eq 7}$$

where, St is the Stokes number;

w is the stage slot width (cm);

L is the stage slot length (cm); and

C is the Cunningham slip correction factor.

As Equation 6 shows, $D_{p,50}$ varies with the dimensions of the slot and the airflow rate. A discussion of St, C and other parameters has been given elsewhere (15).

Another variable of interest regarding the Sierra 210 is the percentage of particle mass in the size range captured by each stage, i.e., $\delta_i = (W_i/W_T) \times 10^2$, where W_i and W_T are the dust masses collected on, say, stage i, and the total mass collected by the cascade impactor, including the back-up filter, respectively. The variable δ_i permits calculation of the percentage (%) cumulative dust mass for every $D_{p,50}$ corresponding to each cascade impactor stage, i.e., Σ_i. Size distribution information, e.g., MMAD and σ_g (geometric standard deviation) can be obtained by plotting Σ_i versus $D_{p,50}$ according to procedures described elsewhere (11).

A similar procedure to the one outlined above, but measuring the α-particle activity on each impactor stage substrate, instead of the dust mass, permits the calculation of the percentage cumulative activity, ΣA_i, for each stage, and hence its corresponding $D_{p,50}$. Activity distribution information, e.g., AMAD and σ_g, can then be obtained by plotting ΣA_i versus $D_{p,50}$ (11).

In summary, the measurement of dust mass, and of its associated α-particle activity, on each cascade impactor stage substrate permits calculation of the MMAD and AMAD, respectively. Figure 18 shows a view of the assembled cascade impactor Sierra 210.

The Sierra 210 can be operated within the approximate airflow rate range of 3 to 20 L/min, depending on the number of impactor stages used and the values for $D_{p,50}$ of interest. The instrument provides data on aerodynamic particle size distributions.

Although portable and not excessively heavy, the Sierra 210 has been designed for laboratory and field work use. A cascade impactor designed for personal use, namely the Marple 290 is described below.

B. Cascade Impactor Marple 290

The Marple 290 is a small, light weight cascade impactor designed for personal use. The device is equipped with a personal mounting bracket so that it can be attached to the person's lapel or pocket. The Marple 290 can operate with 4, 6 and 8 impactor stages followed by a back-up filter. Most of the data reported in the present study have been obtained using 8 stages. On a few occasions, two Marple 290 cascade impactors were used; one of which was operated with only four stages, whereas the other impactor was operated with eight stages. The purpose of this, as will be discussed in due time, was to compare the performance of the Marple 290 with varying numbers of impactor stages. Figure 19 shows pictures of this cascade impactor.

The impactor stages of the Marple 290 have been designed with 6 radial (rectangular) slots, with rounded off edges. The width of the slots decreases for the different stages in the direction of the device's airflow, i.e., largest width at the air inlet and smallest width at the outlet. As previously indicated for the Sierra 210, the width of the slot and the sampling airflow rate of the Marple 290 determines the $D_{p,50}$.

Dust particles entering the cascade impactor are collected on special substrates cut-out to match the impactor stages. Stainless steel, Mylar, and Teflon substrates have been used in the present study.

The Marple 290 can be operated in the airflow range from 0.5 to 5 L/min. However, the best cascade impactor performance is obtained, according to the manufacturer, if operated at approximately 2 L/min. The values obtained for $D_{p,50}$ for the different stages at this airflow rate range from ~0.5 to 21.0 μm, which is the approximate dust particle size range of the device.

Calculation of the $D_{p,50}$ for the different stages of the impactor is

done in a similar fashion as described for the Sierra 210. The same applies to other calculations such as stage dust loading, and so on. As with any other cascade impactor, particle bounce may become a problem, and in this regard some substrate materials have advantages over other materials. Commonly used substrate materials include stainless steel (SS) and mylar (MY). In some cases the use of a special 'impaction' grease is recommended to minimize particle bounce. Usually a toluene solution of the grease is used to coat the substrate and the solvent (toluene) is left to evaporate before the material substrate is used.

A quantity of interest is the effectiveness, E, of the cascade impactor which is defined as:

$$E = e(1 - f) \qquad \text{Eq 8}$$

where, e is the sampling efficiency of the cascade impactor, i.e., the percentage of particles suspended in air that enters the inlet of the impactor; and

f is the internal loss, defined as the percentage or fraction of particles which enter the inlet of the impactor and are collected on extraneous internal surfaces, and not on the collection substrates or back-up filter.

Hence, the corrected particle mass for impactor stage i, i.e., $(W_i)_{corr}$, is obtained by:

$$(W_i)_{corr} = W_i/E \qquad \text{Eq 9}$$

where, W_i is the uncorrected particle mass for impactor stage i.

The variable E increases with decreasing particle size. It is nearly 1 for particles of size less than about 5 μm, but it decreases rapidly for particles of size greater than 5 μm, e.g., for particles of size ~20 μm, E ~0.5 (see Marple 290 instruction manual).

Following identical procedures to those outlined and discussed for the Sierra 210, the cascade impactor Marple 290 allows determination of the MMAD,

AMAD, and their respective geometric standard deviations, σ_g, from particle size distribution plots.

C. The Quartz Crystal Microbalance (QCM) Cascade Impactor Model PC-2

Technological advances in miniaturization, detector design, processing methods and techniques, and other advances have made it possible to design and build fully automated cascade impactors whose means of dust evaluation is different to the traditional method of manual dust mass weighing after air sampling. An instrument whose method of operation departs significantly from the traditional method is the Quartz Crystal Microbalance (QCM) cascade impactor model PC-2. This instrument uses piezoelectric crystals as impactor substrates. Every piezoelectric crystal used in (each) impactor stage has a different natural vibration frequency. Deposition of dust particles on the impactor substrates shift their natural frequencies by an amount proportional to the mass deposited. Automatic measurements of these natural vibration frequency shifts allow (automatic) calculation of dust particle mass on each impactor substrate and rapid particle size distribution calculation by internally implemented software in conjunction with microprocessor-controlled hardware. Because of the sensitivity of the method, complete dust characterization is possible (including sampling) in a time ranging from a few seconds to several minutes, depending on the airborne dust concentration. The instrument is known under the commercial name PC-2 and is manufactured by California Instruments (U.S.A.). In what follows, this instrument will be referred to as QCM or PC-2. Figures 20 to 22 show the instrument and a flow diagram of the experimental set up.

The instrument consists of two sub-assemblies: a sensing stack and a control unit that is detachable (see Figure 20). The cascade impactor of the instrument operates at an air sampling flowrate of 0.24 L/min, and has 10 stages that separate airborne particles into ten 50% efficiency cut-off sizes ($D_{p,50}$) between 0.05 μm and 25 μm. The QCM can accept airborne particle

clouds in a wide concentration range, namely, from 10 $\mu g/m^3$ to 60 mg/m^3. This concentration range can be increased to a few g/m^3 by using an optional high concentration fixed volume sampling valve, model PC-202. For the airflow rate at which the QCM is operated, the $D_{p,50}$ for the different stages are as follows:

Stage	$D_{p,50}$ (μm)
1	25.0
2	12.5
3	6.4
4	3.2
5	1.6
6	0.8
7	0.4
8	0.2
9	0.1
10	0.05

A built-in printer in the control unit displays airborne particulate matter data in two different formats in:

a) histogram format in which the x-axis represents the $D_{p,50}$ corresponding to a given impactor state and the y-axis shows the percentage (%) of the total particle mass accumulated in this stage; and

b) tabular format in which three columns are shown. The 3 columns from left to right show, respectively, the impactor stage number, the shift in natural frequency, Δf, of the crystal corresponding to this stage, and the particle mass concentration (g/m^3) calculated from Δf.

Also shown in the print-out is the sampling time and the total particle mass concentration, which corresponds, as one would expect, to the sum of the concentrations of all the impactor stages.

The mass concentration corresponding to stage i, C_i, is given by:

$$C_i = K_i(\Delta f_i/\Delta t) \text{ in } \mu g/m^3 \qquad \text{Eq 10}$$

where, K_i is a constant, and Δt is the sampling time.

The total particle mass, C_T, is obtained by adding all the stages,

i.e.:

$$C_T = \sum_{i=1}^{10} C_i \qquad \text{Eq 11}$$

The constant K_i in the above expression varies with the impactor stage, e.g., from 3.1 for stage No. 10 to 7.7 for stage No. 1.

Because the QCM measures particle mass as a function of $D_{p,50}$, the data obtained can, in principle, be used to calculate the MMAD. These data are essentially of the same kind as that obtained with the two manually-operated cascade impactors described previously, namely, the Sierra 210 and the Marple 290. The radioactivity associated with the dust deposited on the impactor substrates, i.e., crystals, is very difficult to measure because of:

a) the special crystal mount in the impactor stage assembly (see Figure 22);
b) the small amount of dust collected and required on each stage for accurate dust measurement which is, however, not sufficient for accurate radioactivity measurements.

The user of the instrument should be aware of some practical limitations of the QCM for continuous monitoring. One limitation is crystal saturation which means that a given crystal can only 'tolerate' a certain dust loading for accurate dust measurement before cleaning of the crystal becomes necessary. Typically, the sensitivity of the QCM is 1.4×10^{-9} to 1.5×10^{-9} g/Hz. This means that for every ~1.5×10^{-9} g of dust mass impacted on the sensing crystal's surface, there will be a frequency shift of 1 Hz. The QCM becomes saturated when the dust mass loading versus frequency change relationship is no longer linear. Under favourable conditions, e.g., particles that stick to themselves, the saturation limit is ~2 kHz. Under less favourable conditions this limit is about 500 Hz. Because, on the average, about 3.0×10^{-9} g are necessary for an accurate measurement - which corresponds to 20 Hz frequency shift - a maximum of 25 to 100 complete measurements of airborne dust can be carried out with the QCM before the

crystals need cleaning. The above frequency shifts apply mostly to monodisperse aerosols. For polydisperse aerosols the frequency shift, Δf, should be 35 to 50 Hz. Hence, under these conditions the total number of complete runs before crystal cleaning is reduced from ~15 to less than 60.

However, the special design of the sensing crystal assembly in each impactor stage (see Figure 22) reduces the frequency of crystal cleaning because of the following. Frequency shifts for each impactor stage brought about by dust deposition is effected by two identical unsealed crystals, one used for collecting particulate matter, and the other as the reference crystal. Because of the special and rather unique design of the crystal assembly in each impactor stage, which permits easy flip over and exchange between the crystal sensor and the reference crystal, up to four crystal configurations for each impactor stage are possible before actual crystal cleaning becomes necessary.

CYCLONES

Cyclones are one of the first devices developed for personal dust sampling. Cyclones are mechanical devices of very simple design, and their theory of operation is well understood.

Cyclones consist of a cylindrical or conical chamber, or both, upstream of a filter/filter holder assembly and an air sampling pump. Air is drawn in tangentially near the top of the chamber and is forced to spiral down the outer region of the chamber, reversing its flow at the bottom of the chamber and spiralling up the inner region of the same to an exit tube located at the top of the cyclone chamber. Airborne particles large enough, i.e., with sufficient inertia, are not able to follow the airflow pattern (streamlines) and impact onto the internal walls of the cyclone chamber where those particles are either retained or migrate to the bottom of the cyclone chamber. Dust particles of small enough size are held in the airflow and are deposited in the sampling filter.

Cyclones require careful handling because large particles may deposit on the filter if the device is accidentally overturned. Another concern is the change of the collection characteristics of the cyclone due to wear and tear. This is so because the machining tolerances of cyclones are rather critical. Hence, a change in the physical dimensions brought about by, say, extended use of the device can easily cause a shift in the cut-point characteristics of the cyclone, and hence, of the deposition characteristics of dust on the sampling filter.

The cyclone is, to some extent, a self-correcting device for small changes in the sampling airflow rate. Thus, if the sampling airflow rate, Q, increases, the (top) size-cut of the cyclone will decrease. The net result of an increase in Q followed by a decrease in size cut is that the total dust mass collected will remain the same as before the increase in Q. The converse of the above is equally true, namely, a decrease in Q causes an increase in the cut size leaving the collected dust mass the same as before the decrease in Q.

A variety of electrical charge conducting and non-conducting materials have been used in the construction of cyclones, particularly aluminum (Al), stainless steel (SS), nylon (NY), and other plastic materials. Because dust particles are usually electrically charged and non-conducting materials, e.g., nylon, teflon, PVC, and the like, can easily acquire electrostatic charge, electrical insulators can have a significant effect on the dust collection characteristics of cyclones. The effect of these non-conducting (e.g., insulating) materials is to significantly reduce the dust collection efficiency of the cyclone. Despite this obvious drawback, the pertinent regulatory government agency in the province of Ontario has accepted the use of nylon cyclones as personal dust samplers for occupational exposure calculation purposes.

Although, for the purpose of this study, any suitable filter material

could, in principle, be used, silver membrane filters (25 mm diameter, ~5 μm pore size) were used. This type of filter material offers the advantage of being most suitable for X-ray diffraction analysis of the dust samples. The cyclones used in this study were York nylon cyclones purchased from Levitt Supply (Canada) operated at a nominal airflow rate of 1.8 L/min (see Figure 23).

THE OPEN-FACE FILTER SAMPLER

The open-face filter sampler represents, from the conceptual standpoint, the simplest dust sampler of all mechanical devices. It consists of a suitable filter holder, housing an adequate filter (see Figure 24), operated in conjunction with a sampling air pump. Because the dust collection is effected by an open-face filter configuration, electrostatic effects are not too severe and any filter-holder material can be used, although it is recommended that stainless steel or aluminum filter holders be used. Silver membrane filters were also used in this device to allow for dust mass quantification by X-ray diffraction analysis. A sampling flow rate of 1.8 L/min was used. Because the open-face filter sampler has no particle size cut-off point, i.e., it collects dust within virtually all the airborne sizes available, the dust mass concentration obtained with this simple device should be the largest of all the instruments used. In most cases dust mass quantification for the nylon cyclones and the open-face filter samplers was done by sample (i.e., filter) weighing before and after dust exposure.

(PAD) THE PERSONAL α-PARTICLE DOSIMETER

The PAD consists of a quasi-cylindrically shaped plastic body where a sampling head and an air sampling pump of the turbine type are located (see Figures 25 and 26). The pump is driven by rechargeable batteries that provide electrical power for about 18 h. The batteries are charged in specially designed racks by magnetic induction.

The sampling head includes a filter holder with an 1.2 μm Millipore filter facing a track-etch detector film (see Figure 27). The filter and track-etch detector are separated by four collimators which expose four different areas of the track-etch film to the filter. The exposed areas of the track-etch material are covered with four different thicknesses of an α-particle absorber, i.e., polycarbonate material, to detect α-particles of different energy from ^{222}Rn and ^{220}Rn progeny sampled in the filter. Air is sampled through three small holes located on the body of the sampling head of the device. Details regarding the operation of the PAD (designed by CEA, France) have been amply covered elsewhere and will not be repeated here.

The PAD was designed for personal dosimetry of ^{222}Rn and ^{220}Rn progeny in uranium mines and mills. This device is in mandatory use in France, and is also in extensive use in some uranium mines and mills in Saskatchewan (Canada). However, some interest has recently been shown in the PAD as a radioactive dust (LLRD) sampler. The advantage of using the PAD to quantify LLRD, in addition to its more conventional use in $^{222}Rn/^{220}Rn$ progeny assay for dose exposure calculation purposes, is immediately obvious, namely, the most important airborne radioactivity components in uranium mines and mills could be obtained by means of a single device. However, this requires a detailed study of the dust collection characteristics of the PAD.

Except for a small number of cases, the sampling time used for dust monitors of the manually-operated grab-sampling type, such as the cascade impactors, the nylon cyclones, and the open-face filter samplers, was about 8 h or slightly less. This sampling time was sufficient for these devices because, as previously indicated, they were operated at airflow rates ranging from 1.8 L/min to 20 L/min. However, because of the low sampling airflow rates of the PADs (~3.4 L/h), their total sampling times had to be extended significantly in order to collect enough dust mass for reasonably accurate estimations of airborne dust mass concentration. For this reason, the PADs

were used, on average, for 5 'sampling' days at a time. Each day the PADs sampled air together with the devices indicated above for the same period so that direct comparison could be made at the end of the experiment between the PADs and other instrumentation.

OPTICAL PARTICLE COUNTERS

Two optical particle counters were tested in this study, namely, the MiniRam PDM-3, manufactured by GCA Corporation, U.S.A., and the Climet CI-7300, manufactured by CLIMET, U.S.A. A brief description of their principle of operation is given below.

A. The MiniRam PDM-3

The MiniRam, Model PDM-3, is a short name for Miniature Real-time Aerosol Monitor. This instrument is a very compact personal airborne dust monitor which detects dust particles by scattering of electromagnetic radiation in the near infrared (~880 nm wavelength). The monitor uses a pulsed GaAlAs light emitting source which emits a narrow-band 'beam' (half-power bandwidth : 80 nm) of near infrared 'light' of 880 nm wavelength. The average output power of the source is 2 mW. The electromagnetic radiation scattered by airborne dust particles in a 'sensing volume' is detected over an angle of 45^{o} to 95^{o} from the forward direction by means of a Si-photovoltaic hybrid detector in conjunction with a low-noise preamplifier.

The MiniRam is a forward light scattering dust monitor of the nephelometric type; in other words, the monitor detects the combined scattering from the dust 'cloud' present within its ~3 cm^3 sensing volume whose dimensions are large compared with the average separation between the individual airborne dust particles.

The MiniRam has been designed to respond preferentially in the particle size range of 0.1 to 10 μm in order to ensure good correlation with standard gravimetric measurements of both the respirable and thoracic deposition fractions.

An advantage of direct light scattering dust detection is that the rate at which air passes through the sensor does not affect the actual dust concentration measurement. This is so because particle detection is performed directly on every 'parcel' of air going through the constant sensing volume of the device.

The MiniRam can be operated in a purely passive mode, i.e., no use of the sampling air pump is necessary, or alternatively, by drawing air through the sampling (sensing) volume by means of a suitable air sampling pump operated in the airflow rate range of 0.5 to ~2 L/min. Furthermore, the MiniRam is equipped with optional accessories for applications requiring particle precollection, i.e., using a cyclone upstream of the sensing volume to remove particles larger than a given size dictated by the dimensions of the cyclone and the airflow rate of the sampling pump. Depending on the type of study performed, the MiniRam has been used in both modalities, namely, passive mode, as well as in the active mode, i.e., using an air sampling pump, with or without an upstream dust size preselector such as a nylon cyclone. These different options have also been used to compare the response of the instrument to the same dust atmosphere. The several arrangements of the device are shown in Figures 28 to 30.

The MiniRam is provided with a connector jack for printing-out dust concentration data every minute. An external printer designed to operate, or compatible with, the MiniRam can be used. In our case, the printer used was purchased from the same manufacturer that designed the monitor. The MiniRam measures the concentration of dust continuously calculating an average value of this concentration every 10 seconds. After each minute, data is transmitted from the MiniRam to the printer which prints the six average concentration values calculated during this 1 min monitoring time.

The MiniRam also incorporates an interesting and practical feature, namely, it provides the Time-Weighted-Average (TWA) during the measurement

mode up to the instant the key labelled TWA on the front of the instrument is pressed. The TWA is defined as:

$$TWA = (1/t) \int_0^t C(t)dt \qquad \text{Eq 12}$$

where, in the above expression C(t) represents the instantaneous dust concentration at time t measured by the instrument. Another interesting feature of the MiniRam intended for field use is the Shift-Average Dust Concentration (SA) which is automatically calculated by the instrument when the key labelled SA is pressed. The SA is given as the TWA for t = 480 min, i.e., 8 hour work shift.

Although the instrument normally operates in the 0 to 9.99 mg/m^3 dust concentration range, whenever a dust concentration level exceeds the value 9.99 mg/m^3 the MiniRam automatically switches to a higher dust concentration range, namely, 0 to 99.9 mg/m^3 until a new dust concentration level lower than 9.99 mg/m^3 occurs, in which case the instrument reverts to its lower range display and mode (i.e., 0 to 9.99 mg/m^3).

Although the external printer option has always been used in our measurements, in a majority of cases a light-weight, small data acquisition board, under the general commercial name of TELOG, has also been used to store data from the MiniRam for further processing. More specifically, the data stored in the TELOG's memory can be 'dumped' into a PC, IBM-compatible, computer under Spreadsheet, and/or other software which permits trend and statistical analyses, as well as a graphical representation, to be conducted.

A serious problem encountered in the use of the MiniRam has been dust contamination of the optical system. As a result, the 'background' level steadily increases from the beginning to the end of dust sampling causing serious dust concentration estimation errors if corrective measures are not taken. This usually involves frequent 'zero' or 'background' readings of the instrument. This subject will be dealt with in more detail elsewhere.

B. The Climet CI-7300

The Climet model CI-7300, manufactured by CLIMET Instruments Co., U.S.A., is another light scattering particle sizer. The instrument is a microprocessor-based six channel particle counter which uses a quartz-halogen light source and particle light scattering through a wide angle range from 15° to 150°. The standard sampling flow rate is ~28 L/min. The instrument used in the studies presented here operates at a nominal flow rate of 2.8 L/min, and counts dust particles in six particle size ranges with range thresholds at 0.3 μm, 0.5 μm, 0.7 μm, 1.0 μm, 5.0 μm, and 10 μm. The particle size ranges in the instrument are 0.3 to 0.5 μm, 0.5 to 0.7 μm, 0.7 to 1.0 μm, 1.0 to 5.0 μm, 5.0 to 10 μm, and particle sizes greater than 10 μm. The particle size ranges, as well as the airflow rate of the instrument are set at the factory. The sampling airflow rate determines the maximum particle concentration that the instrument is capable of measuring. In general, the maximum particle concentration that the instrument can measure reliably within a given particle size range increases with decreasing operating sampling flowrate.

The CI-7300 is equipped with temperature and relative humidity probe, air velocity probe, thermal printer, RS-232 serial port, analog and digital outputs, and interfaces to control multiport samplers. A number of other optional accessories and features are also available for the instrument. Data are printed-out in a differential count or integral count formats. The instrument is fully programmable; the following variables can be chosen at will to suit particular experimental purposes, e.g., sampling time, interval time between consecutive sampling periods, and cycle delay time. The size sensitivity of the instrument is 0.3 μm, and the particle size resolution is ~0.02 μm. Optional outputs (printed-out data) include temperature, relative humidity and air velocity.

Processing of the particle counts obtained in the 6 particle size

ranges available in the instrument permits particle size distribution to be calculated. Furthermore, if the particle size ranges are properly chosen, the corresponding particle concentrations in these size ranges can be used to estimate a quantity similar to the MMAD, i.e., the mean particle size (MPS) of the dust distribution can be calculated.

Instruments that either do not permit dust mass collection or what amounts to the same, namely, particle collection on (suitable) substrates are still very useful in LLRD characterization because the AMAD is, in principle, closely related to the MMAD or MPS. Hence, knowledge of the MMAD or MPS can be used to infer the AMAD of the LLRD dust cloud investigated. Once such instrument that does not collect particulate matter on substrates, although permitting the calculation of the MPS of the dust size distribution, is the Climet CI-7300. Figures 31 and 32 show, respectively, an overview of the instrument and some details of the air sampling and optical systems.

REFERENCES

1. Prodi, V., Mularoni, A., "Electrostatic lung deposition experiments with humans and animals"; Ann Occup Hyg, vol 29, pp. 229-240, 1985.

2. Johnson, J.R., "A review of the dosimetry from inhalation of long-lived alpha-activity in ore dust"; Proc Int Conf on Occupational Radiation Safety in Mining, H. Stocker (Ed.), The Canadian Nuclear Association, (Toronto), vol. 2, pp. 495-502, 1984.

3. McGuive, S.A., "The NRC's limit on intake of uranium ore dust"; USNRC Report NUREG-0941, Washington, D.C. 20555, U.S.A., Nuclear Regulatory Commission, 1983.

4. Duport, P.J. and Edwardson, E., "Characterization of radioactive long-lived dust present in uranium mine and mill atmospheres"; Proc Occupational Radiation Safety in Mining, H. Stocker (Ed), The Canadian Nuclear Association, (Toronto), vol. 1, pp. 189-195, 1985.

5. Knuth, R.H. and George, A.C., "Uranium mill ore dust characterization"; Report EML-384, Environmental Measurement Laboratory, Department of Energy, EML, 1980.

6. Paschoa, A.S., Wrenn, M.E., Singh, N.P., Miller, S.C., Bruenger, F.W., Jones, K.W., Cholewa, M. and Hanson, A.L., "Uranium bearing particles in miners' and millers' lungs"; Proc Occupational Radiation Safety in Mining, H. Stocker (Ed), The Canadian Nuclear Association, (Toronto), vol. 2, pp. 511-517, 1984.

7. National Research Council, "Measurement and control of respirable dust in mines"; N.G.W. Cook (Ed), (NMAB-363). Washington, D.C., National Academy of Sciences, pp. 1-388, 1980.

8. Walton, W.H., (Ed), Inhaled Particles III; Surrey, U.K., Unwin Brothers Ltd., vol. 1, pp. 33-138, 1971.

9. Walton, W.H. (Ed), Inhaled Particles IV; Oxford, Permagon Press, pp. 3-75 and 107-237, 1977.

10. Walton, W.H. (Ed), Inhaled Particles V; (The Annals of Occupational Hygiene, Oxford, Pergamon Press, vol. 26, No. 1-4), Oxford, Pergamon Press, pp. 47-163 and 179-347, 1982.

11. Bigu, J. and Grenier, M.G., "Characterization of radioactive dust in Canadian underground uranium mines"; Proc 2nd Ventilation Congress, P. Mousset-Jones (Ed), Reno, Nevada. A.A. Balkema, Rotterdam, pp. 269-277, 1985.

12. The International Commission on Radiological Protection (ICRP), "Limits for intakes of radionuclides by workers"; by the Committee of the ICRP (ICRP Publication 30, Part 1 and Supplement to Part 1). Oxford, Pergamon Press, pp. 1-555, 1979.

13. The International Commission on Radiological Protection (ICRP), "Radiation protection in uranium and other mines"; by the Committee of the ICRP (ICRP Publication 24). Oxford, Pergamon Press, 1977.

14. The International Commission on Radiological Protection (ICRP), "1990 recommendations of the ICRP"; by the Committee of the ICRP (ICRP Publication 60, vol. 21, No. 1-3). Oxford, Pergamon Press, 1991.

15. Bigu, J., "A review of airborne particle sampling with special reference to Long-Lived Radioactive Dust"; Report submitted to the AECB in compliance with Contract No. 4.108.1, entitled: "Comparison of Radioactive Aerosol Sampling Instruments", Phase I, 1990.

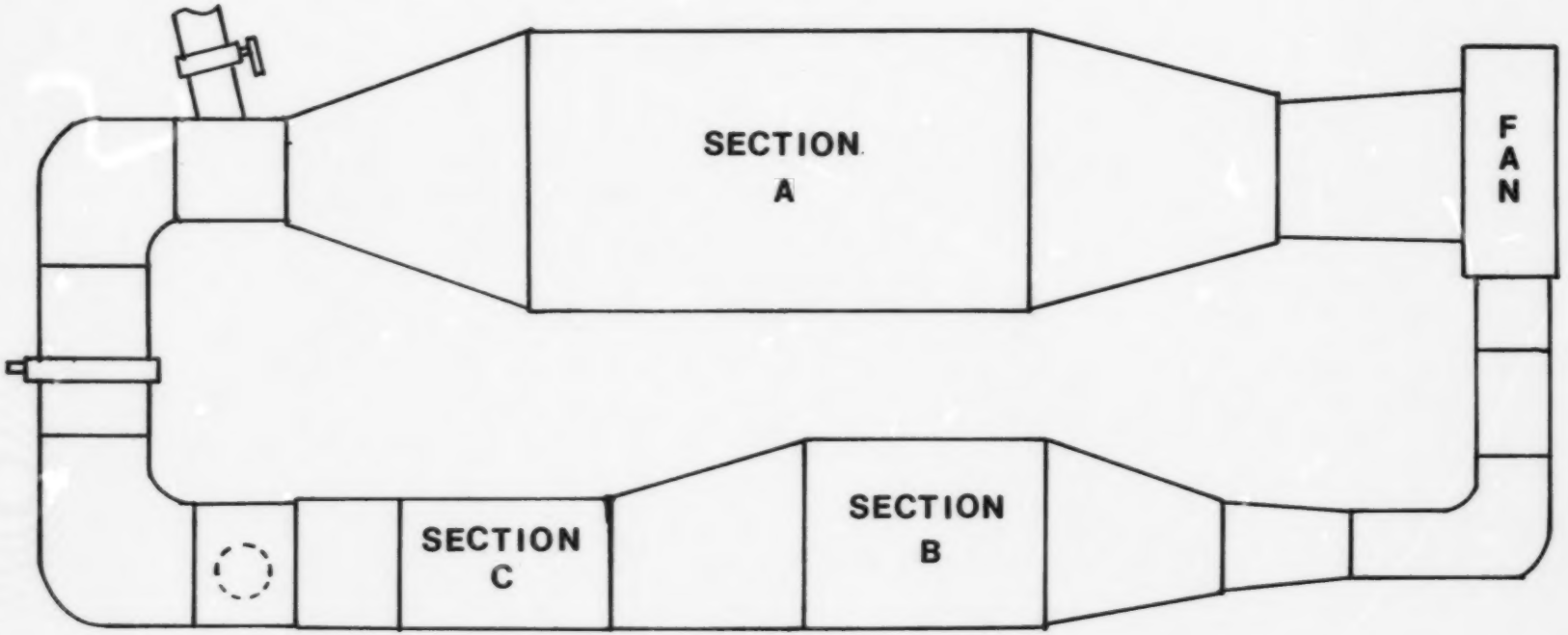

Fig. 1 - Simplified view of the Long-Lived Radioactive Dust Test Facility (LLRDTF).

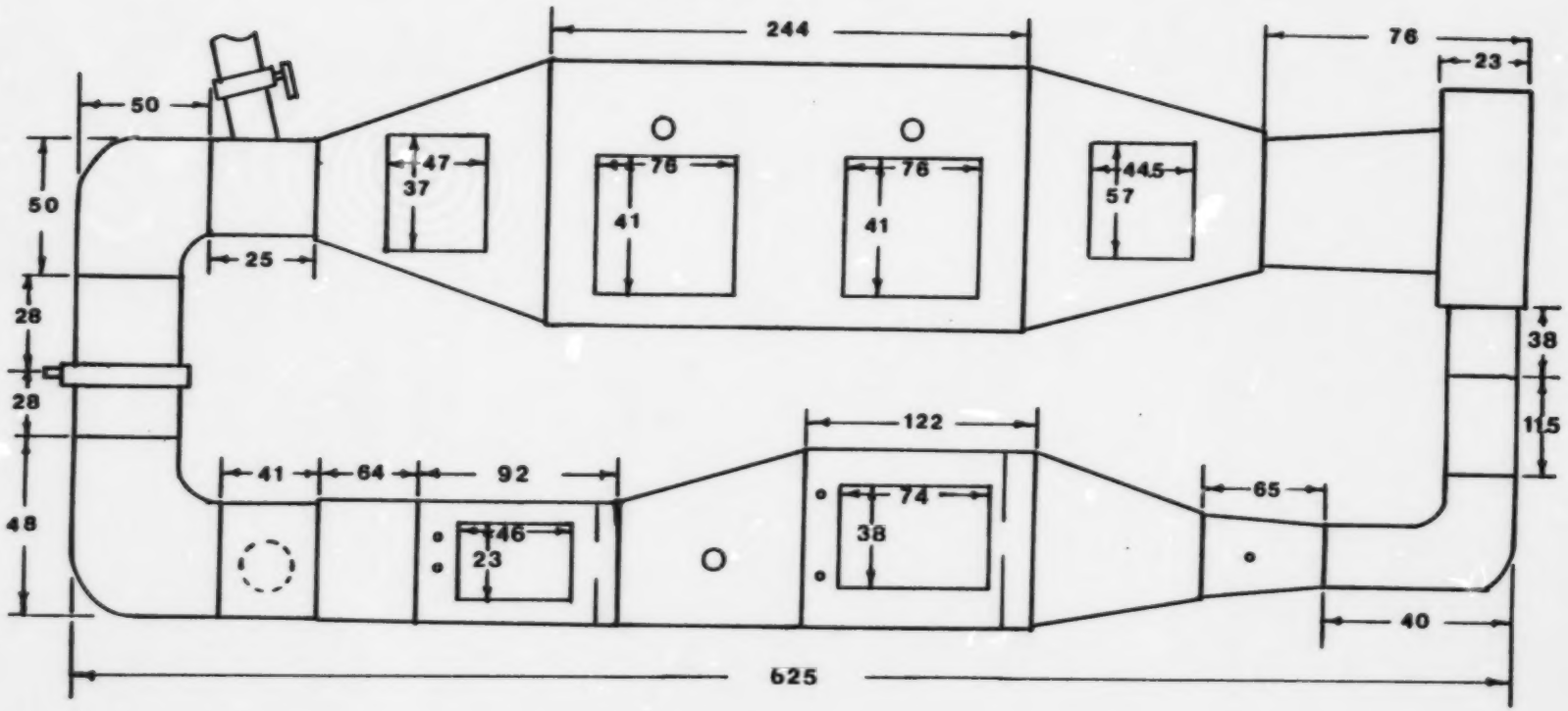

Fig. 2 - Front view of the LLRDTF showing windows, doors, sampling ports and other components.

REAR VIEW

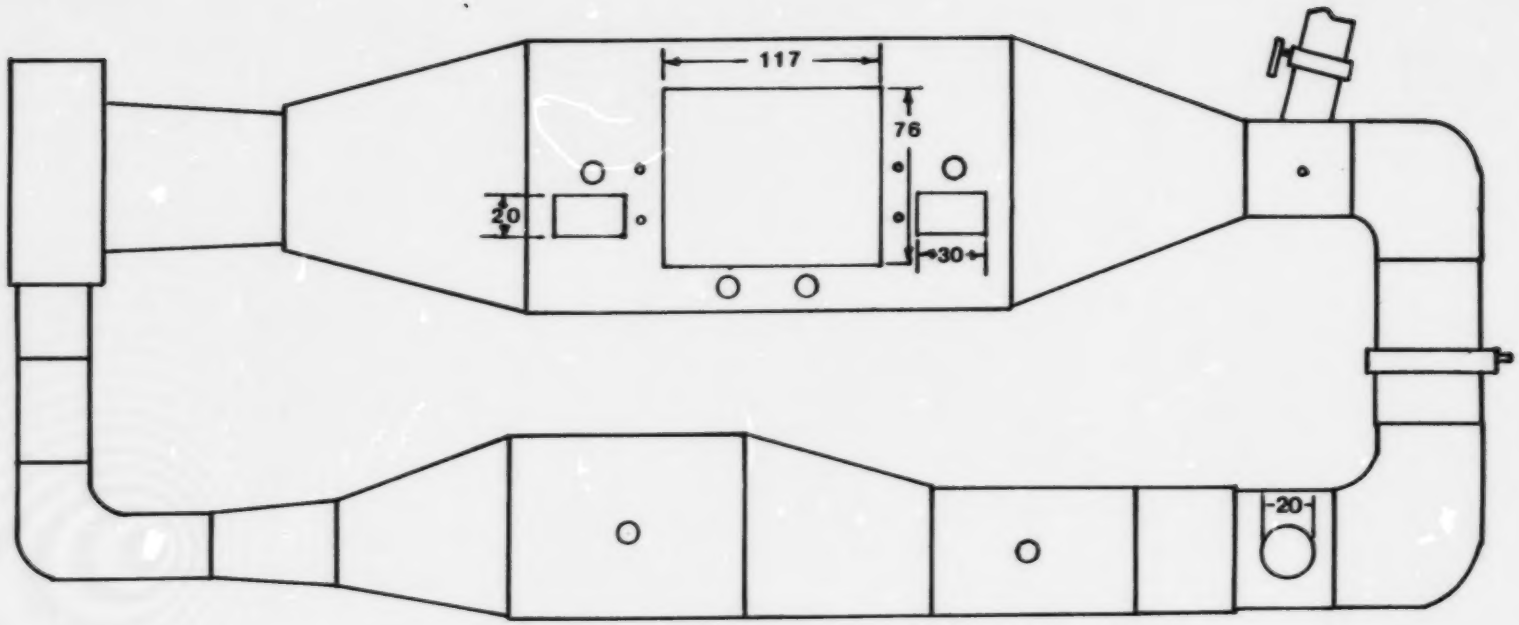

· All dimensions in centimeters
• 1 cm. sampling port with valve
O 4 cm. sampling port

Fig. 3 - Rear view of the LLRDTF showing windows, doors, sampling ports and other components.

TOP VIEW

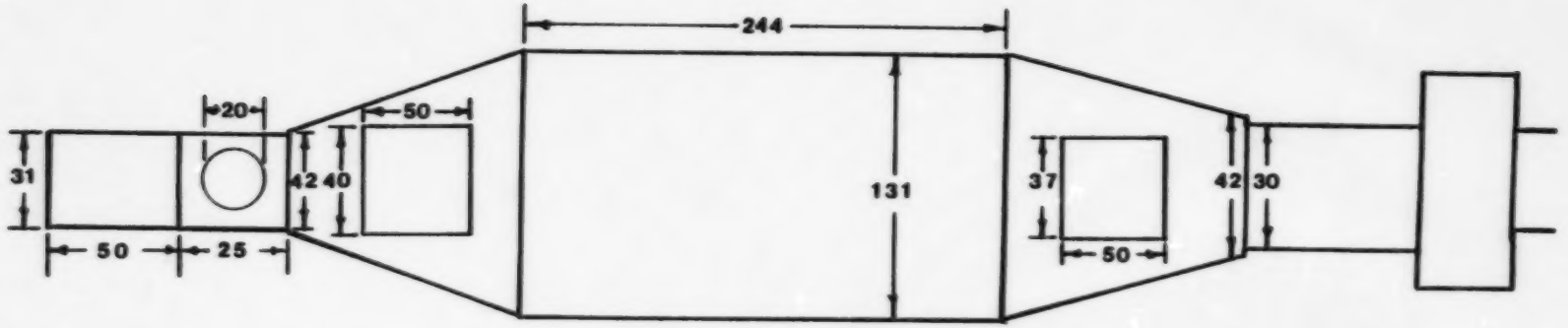

UPPER CHAMBER

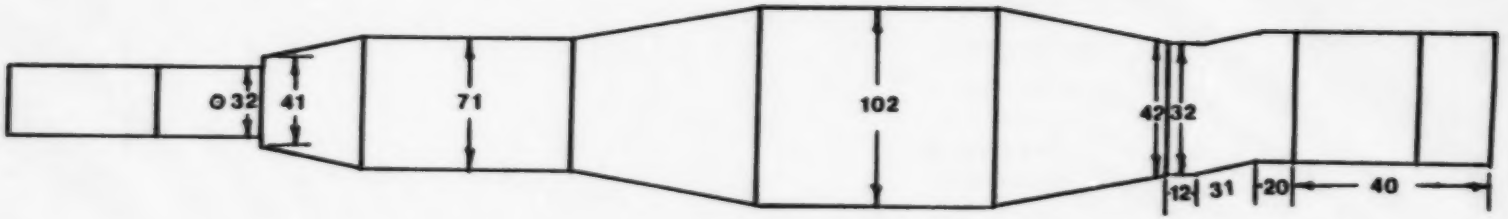

LOWER CHAMBERS

·All dimensions in centimeters

∘ 1 cm. sampling port with valve

O 4 cm. sampling port

Fig. 4 - Top view of the LLRDTF showing windows, sampling ports, valves, and other components.

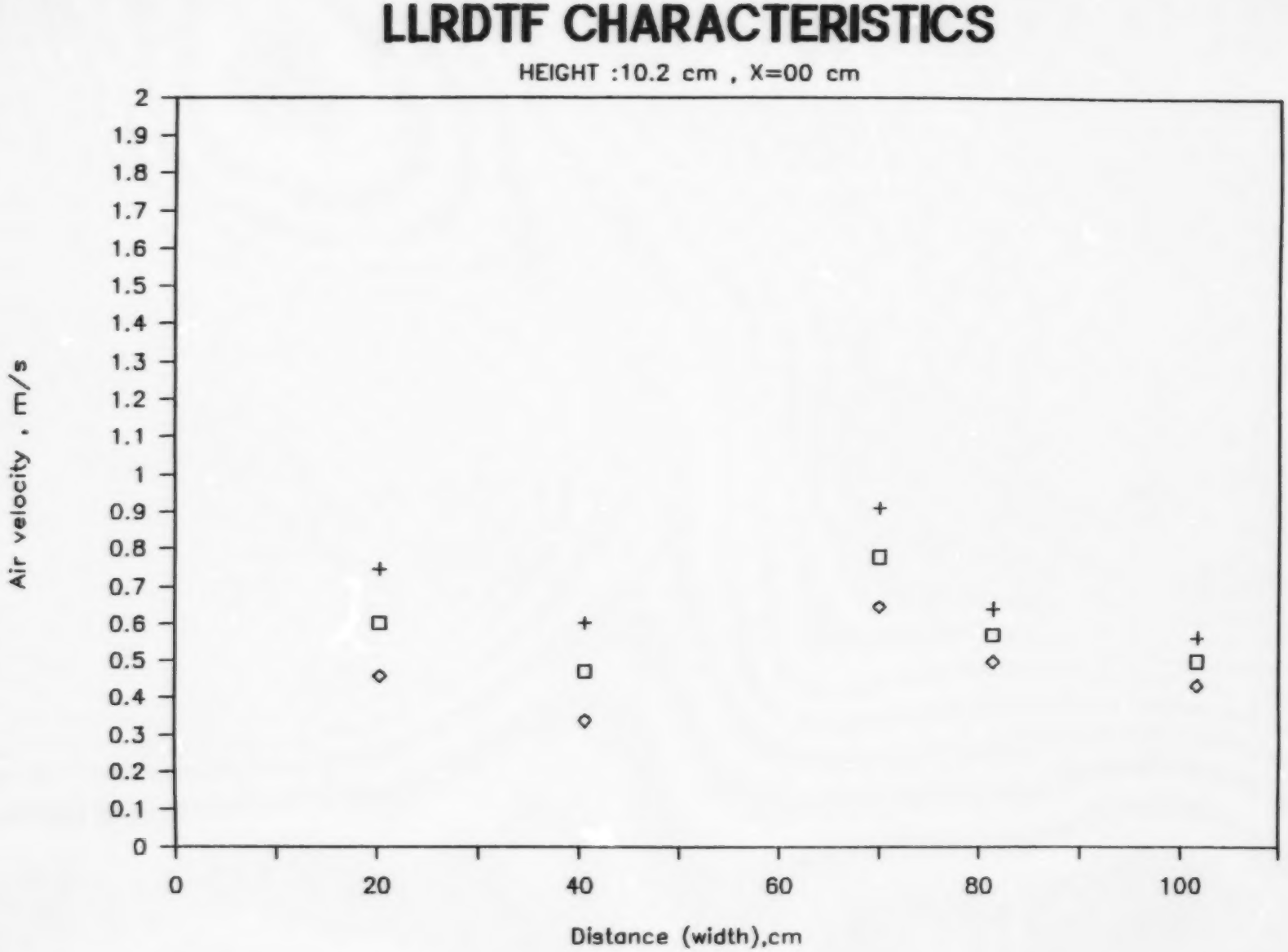

Fig. 5 - Air velocity versus width in section A (S.A) of the LLRDTF for a fixed height (10.2 cm) and distance (0 cm) from the opening of S.A.

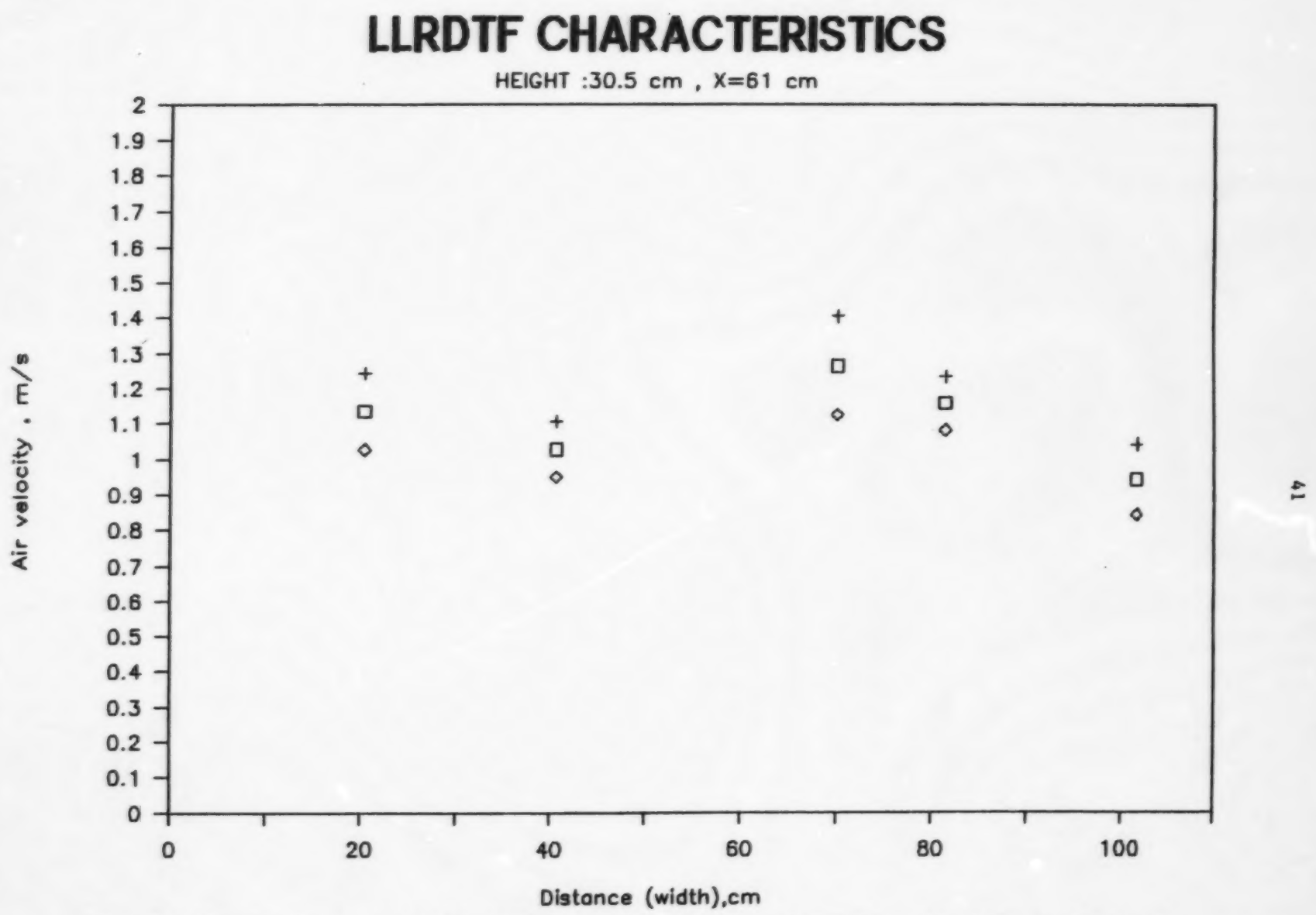

Fig. 6 - Air velocity versus width in Section A (S.A) of the LLRDTF for a fixed height (30.5 cm) and distance (61 cm) from the opening of S.A.

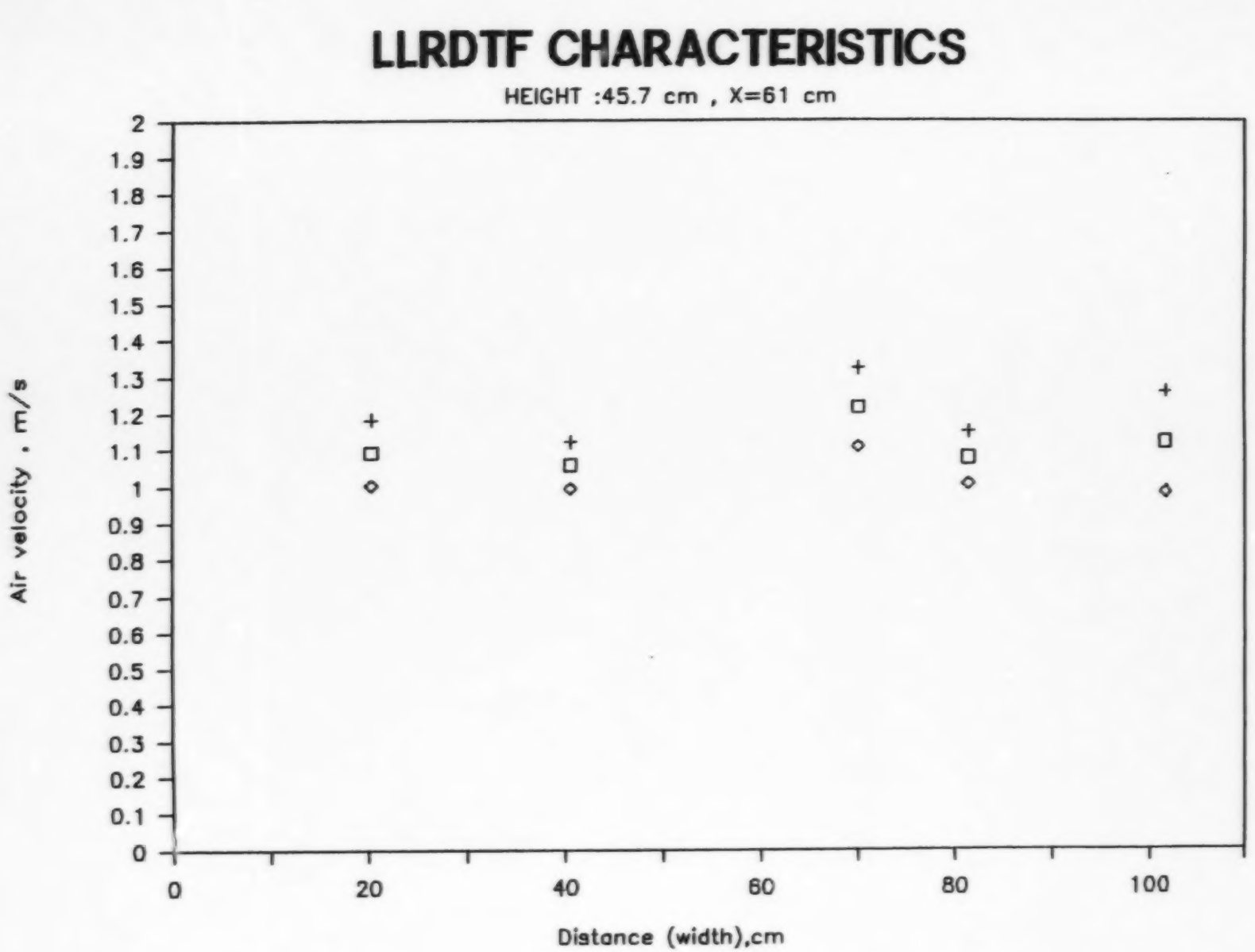

Fig. 7 - Air velocity versus width in section A (S.A) of the LLRDTF for a fixed height (45.7 cm) and distance (61 cm) from the opening of S.A.

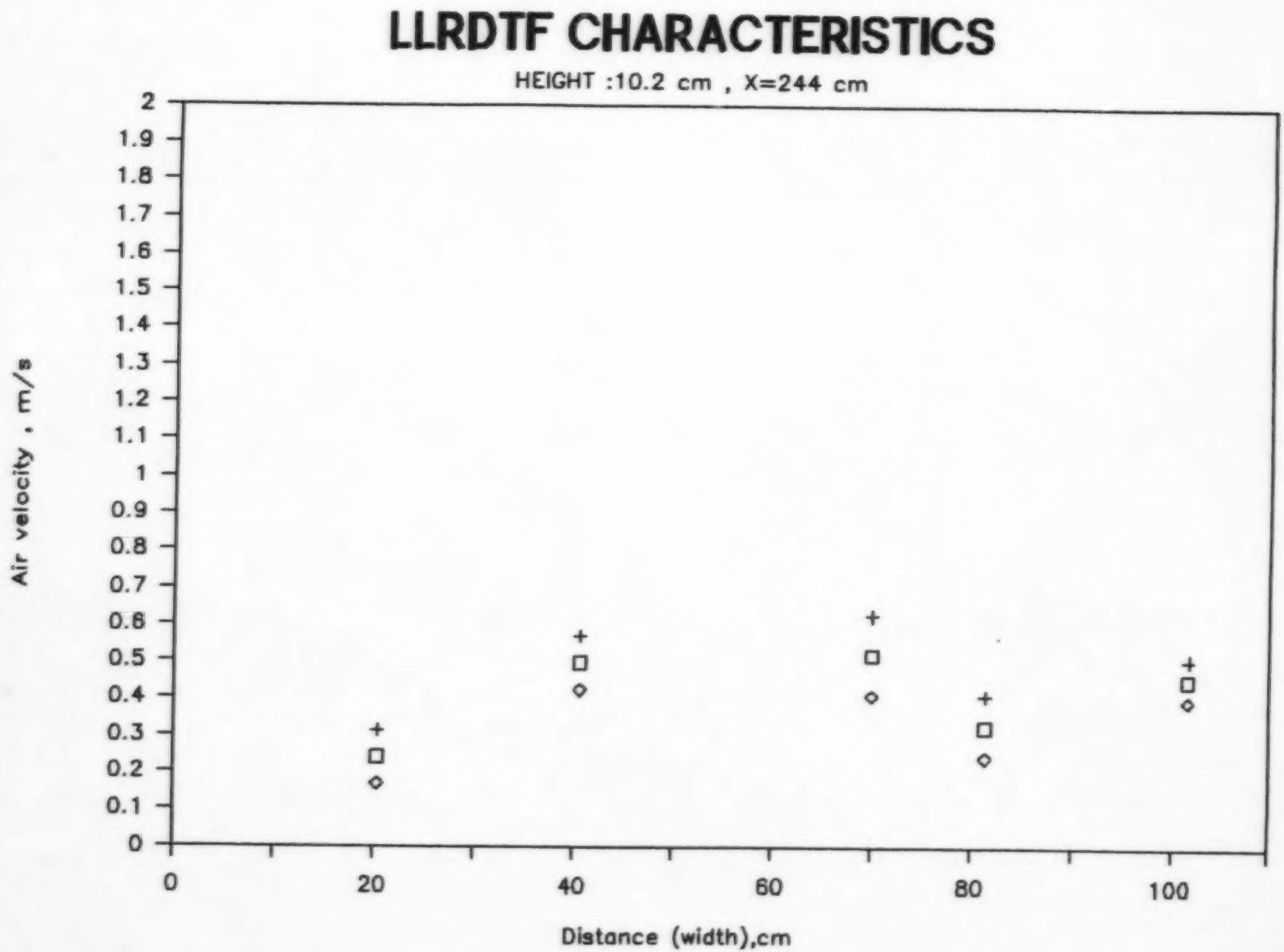

Fig. 8 - Air velocity versus width in section A (S.A) of the LLRDTF for a fixed height (10.2 cm) and distance (244 cm) from the opening of S.A.

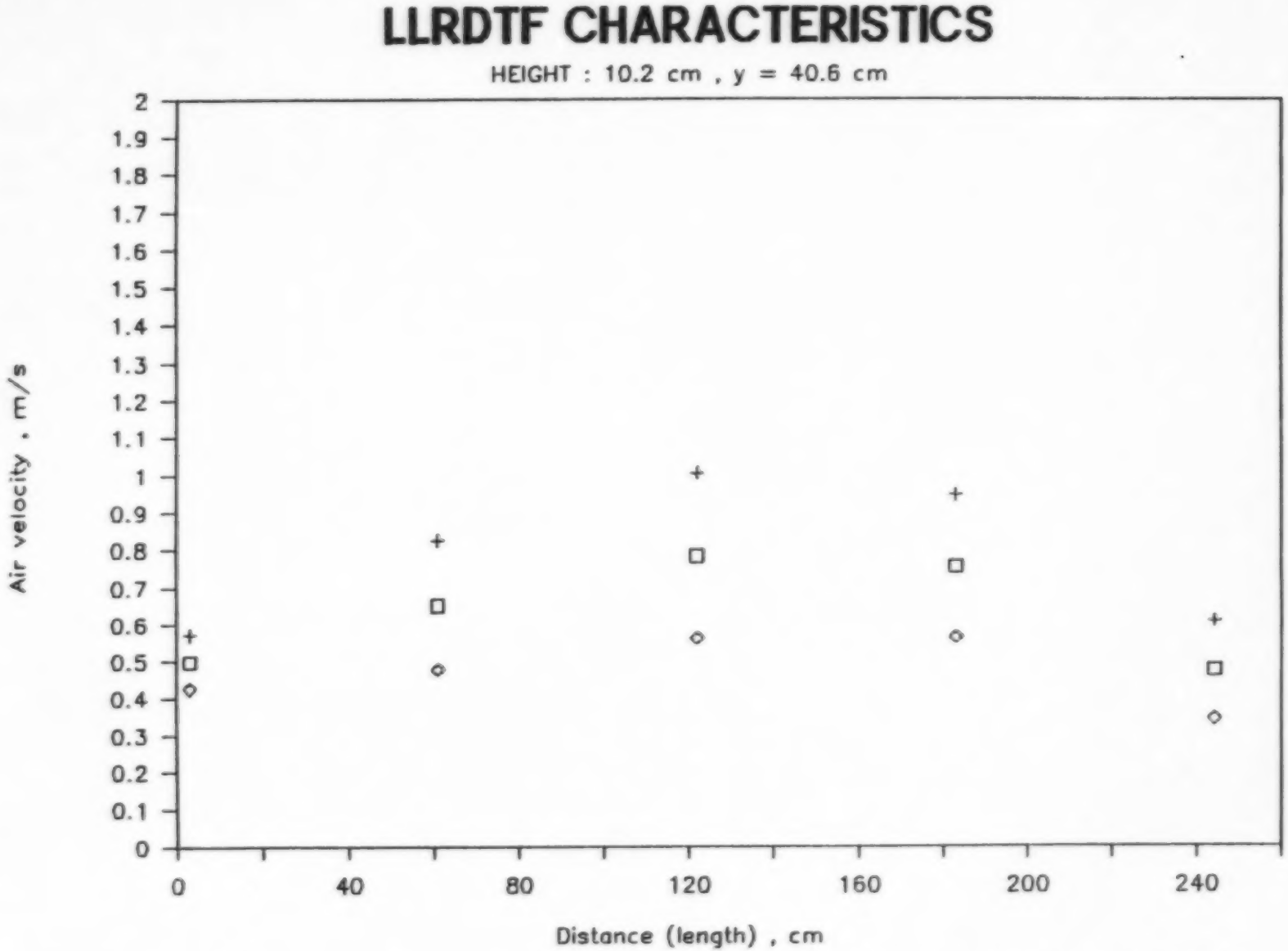

Fig. 9 - Air velocity versus distance from the opening of section A (S.A) for a fixed height (10.2 cm) and width (40.6 cm) of S.A.

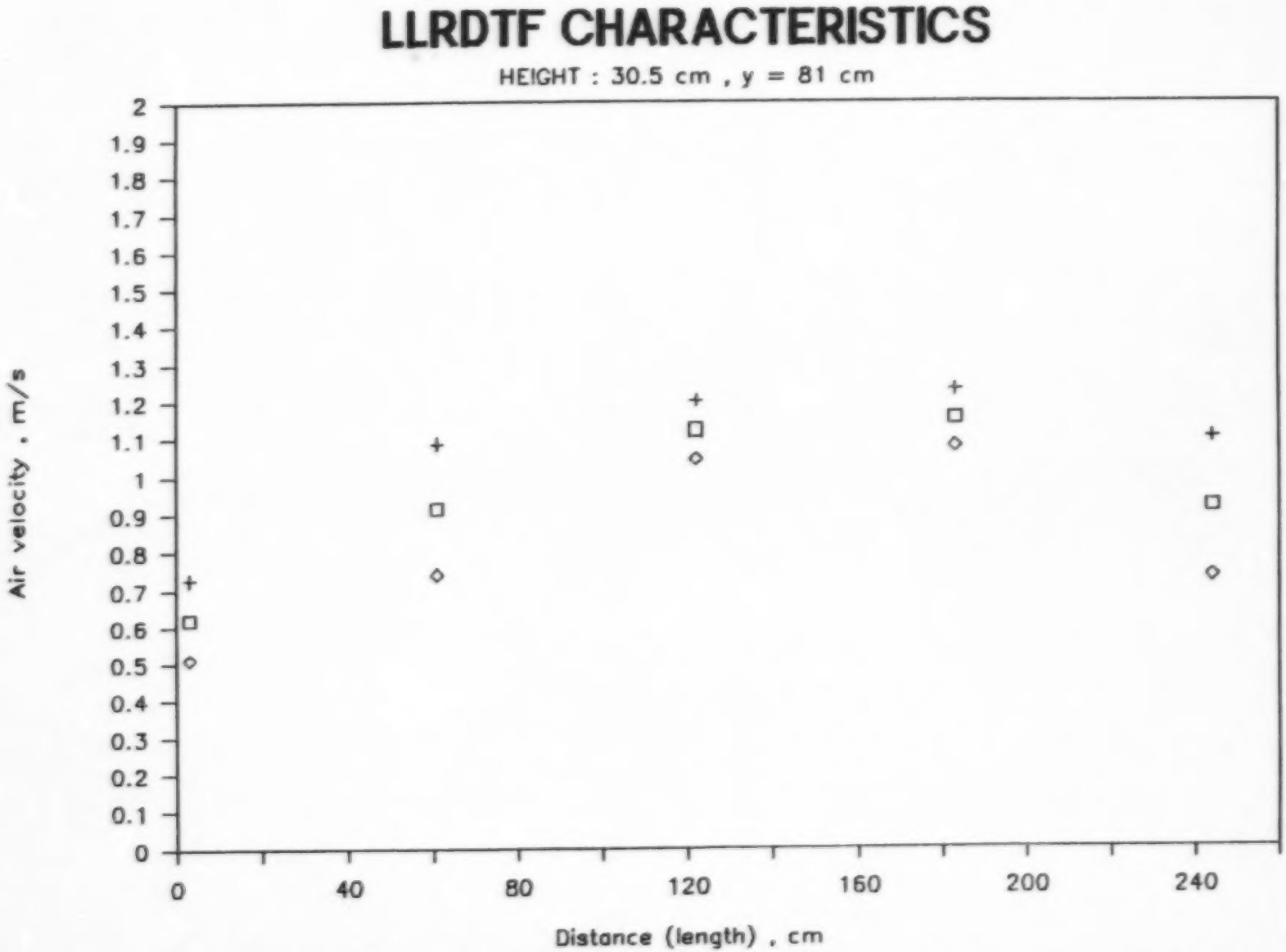

Fig. 10 - Air velocity versus distance from the opening of section A (S.A) for a fixed height (30.5 cm) and width (81 cm) of S.A.

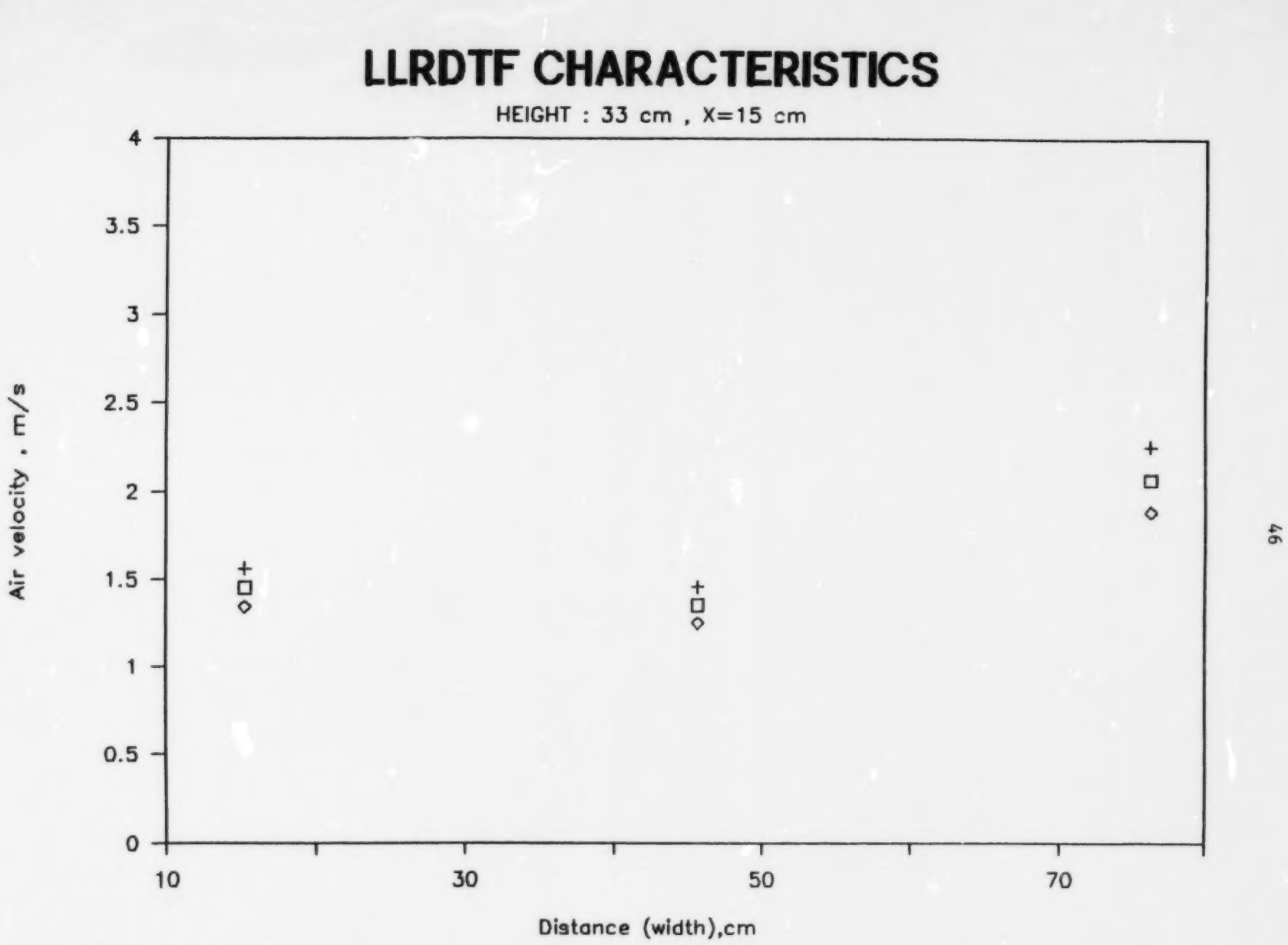

Fig. 11 - Air velocity versus width in section B (S.B) of the LLRDTF for a fixed height (33 cm) and distance (15 cm) from the opening of S.B.

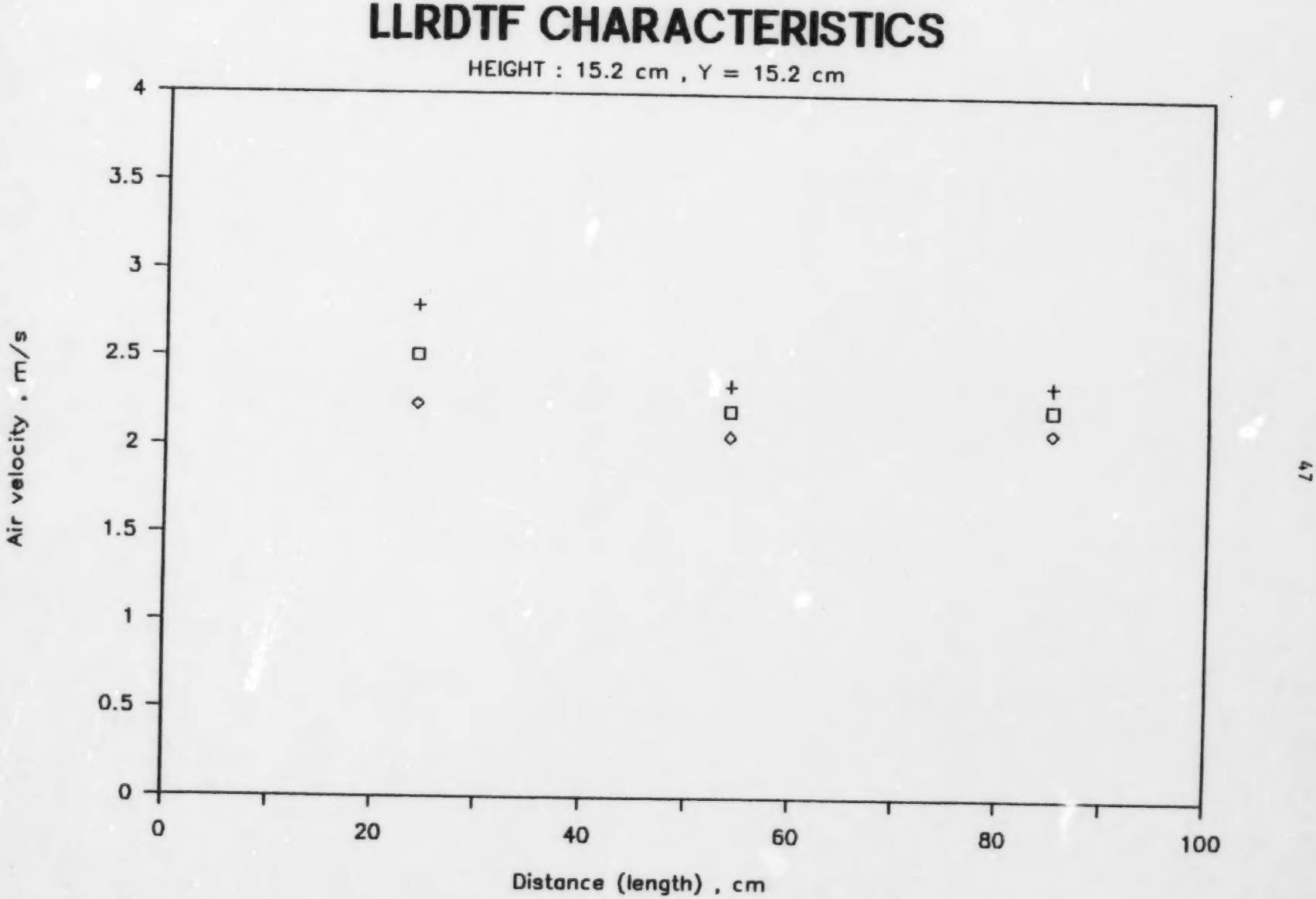

Fig. 12 - Air velocity versus distance from the opening of section B (S.B) for a fixed height (15.2 cm) and width (15.2 cm) of S.B.

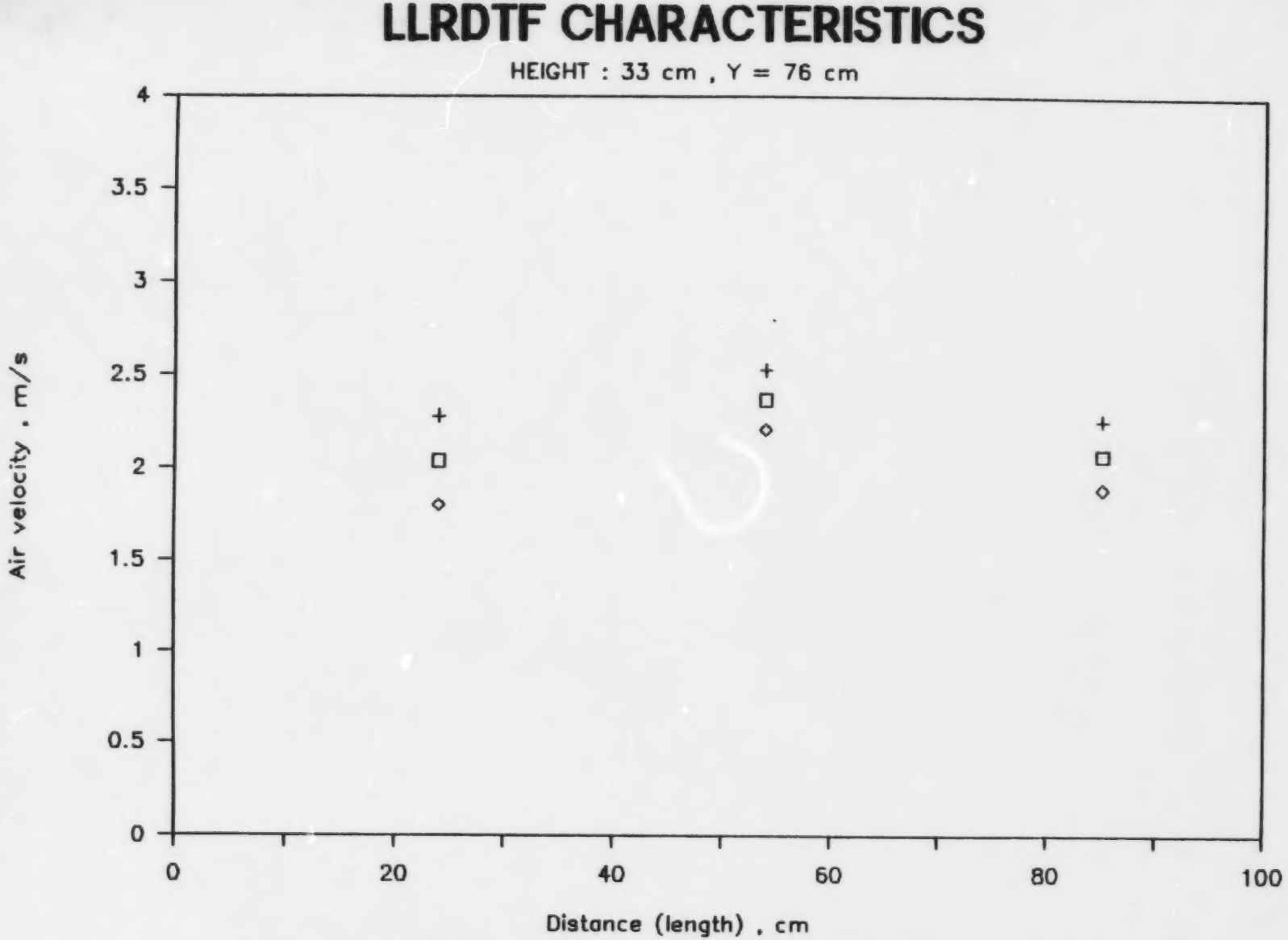

Fig. 13 - Air velocity versus distance from the opening of section B (S.B) for a fixed height (33 cm) and width (76 cm) of S.B.

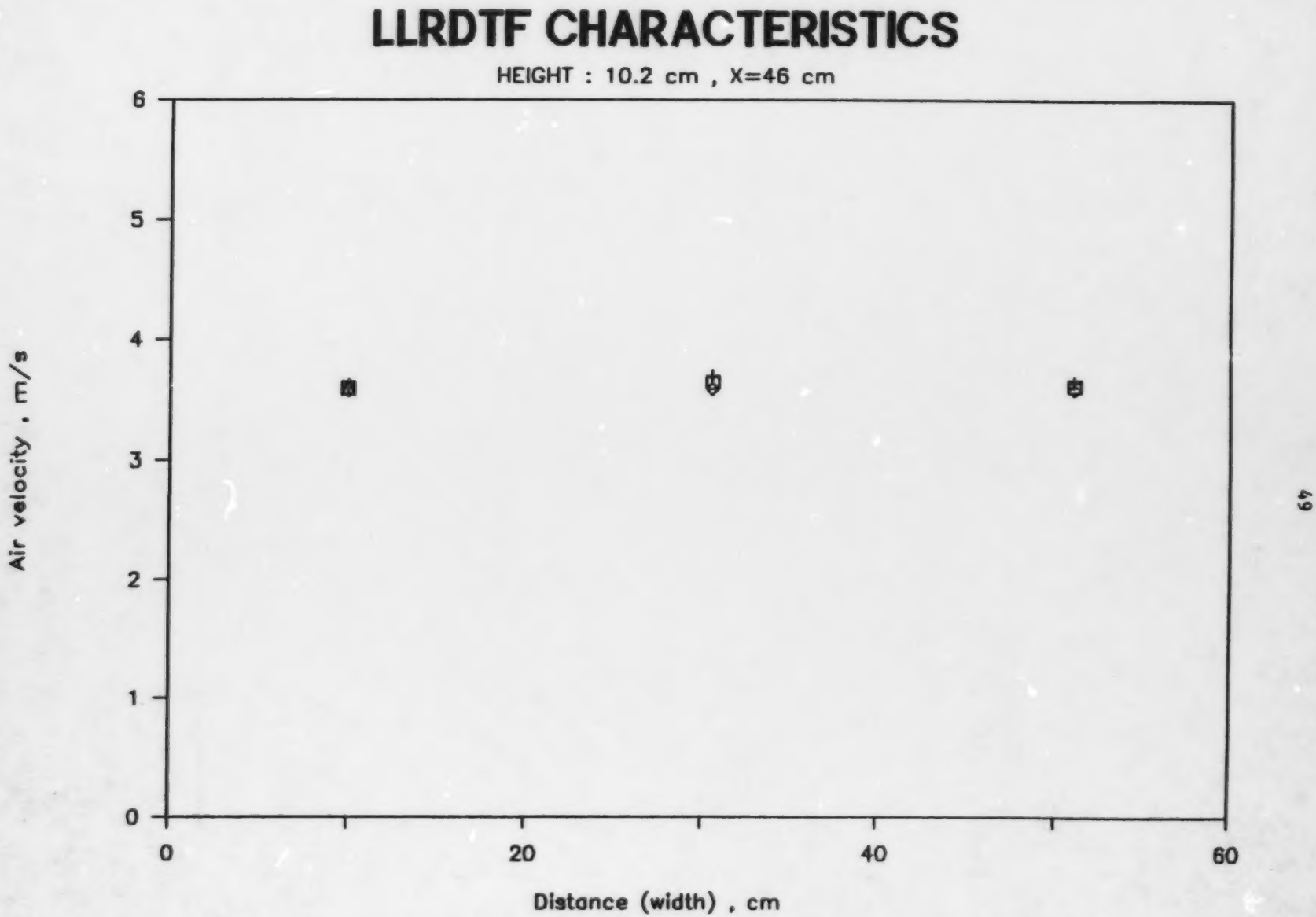

Fig. 14 - Air velocity versus width in section C (S.C) of the LLRDTF for a fixed height (10.2 cm) and distance (46 cm) from the opening of S.C.

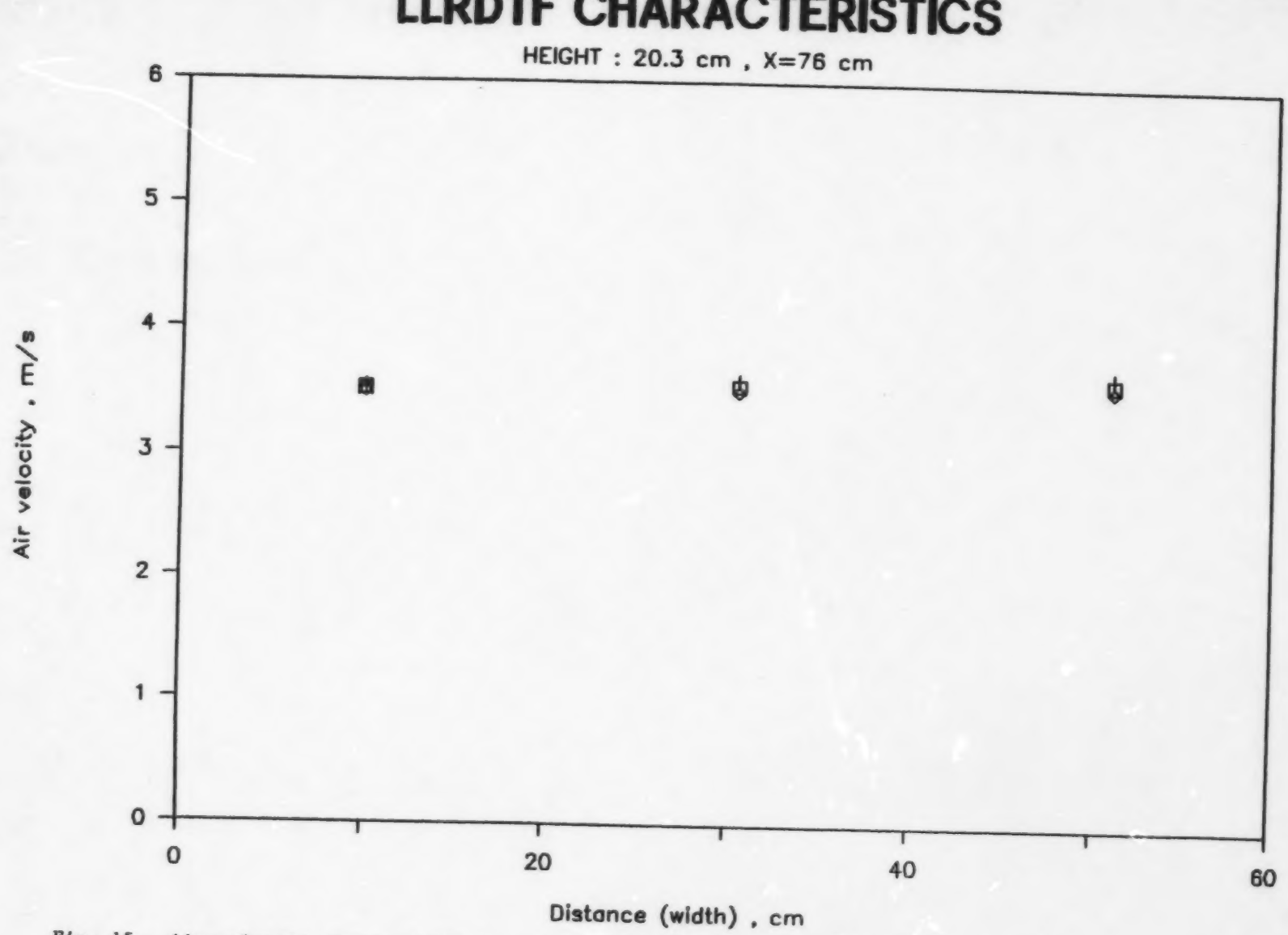

Fig. 15 - Air velocity versus width in section C (S.C) of the LLRDTF for a fixed height (20.3 cm) and distance (76 cm) from the opening of S.C.

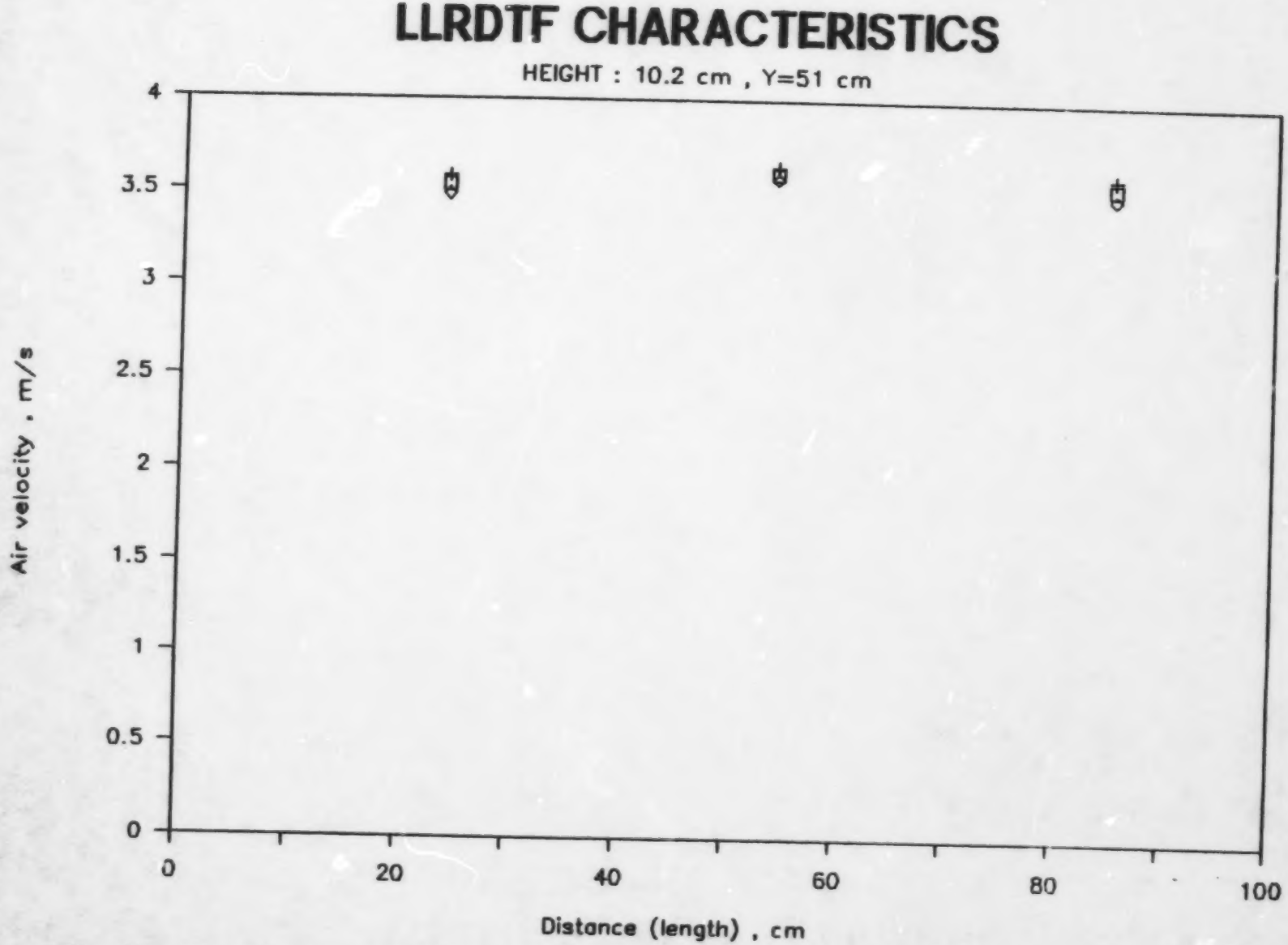

Fig. 16 - Air velocity versus distance from the opening of section C (S.C) for a fixed height (10.2 cm) and width (51 cm) of S.C.

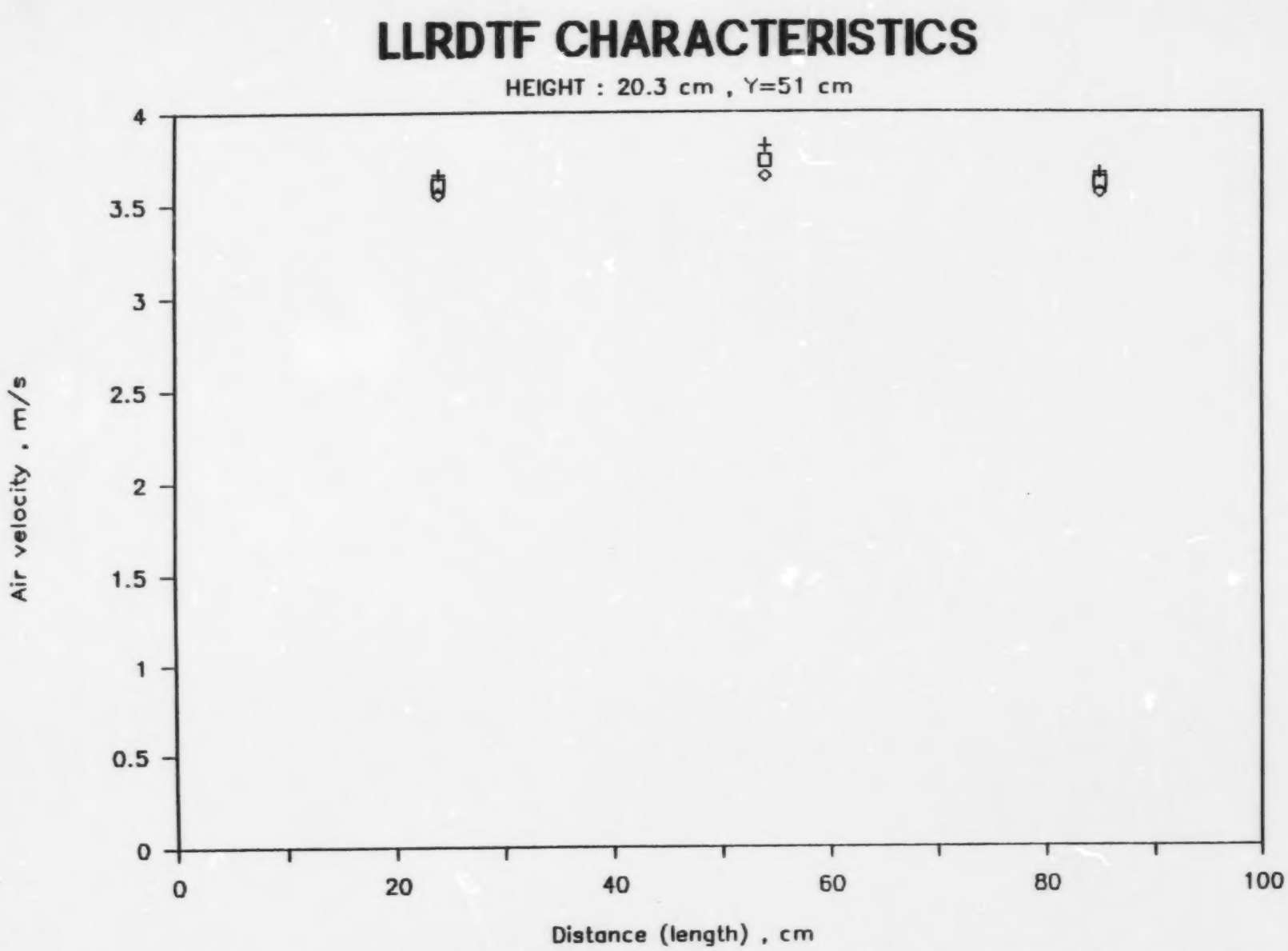

Fig. 17 - Air velocity versus distance from the opening of section C (S.C) for a fixed height (20.3 cm) and width (51 cm) of S.C.

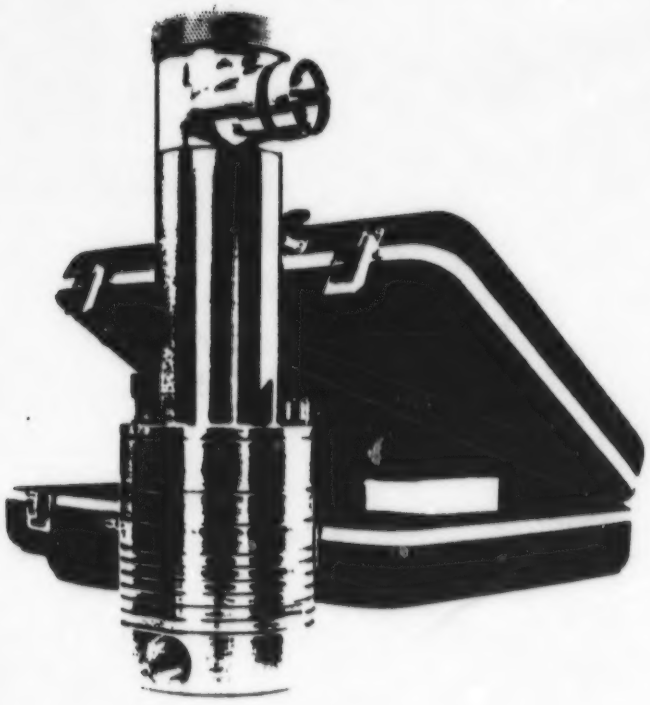

Fig. 18 - view of cascade impactor Sierra 210.

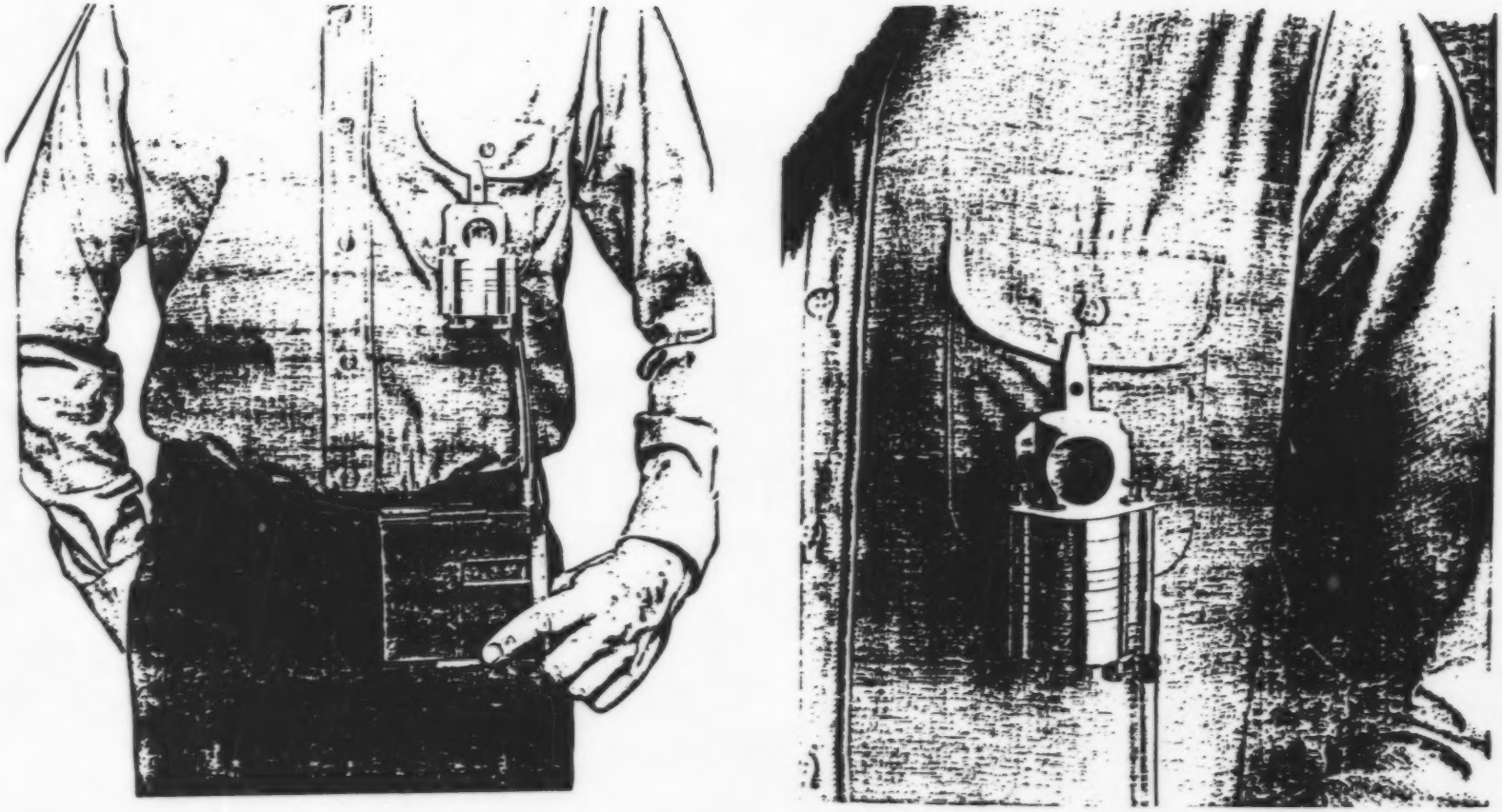

Fig. 19 - View of the cascade impactor Marple 290 with sampling pump (left hand side) and without the pump (right hand side).

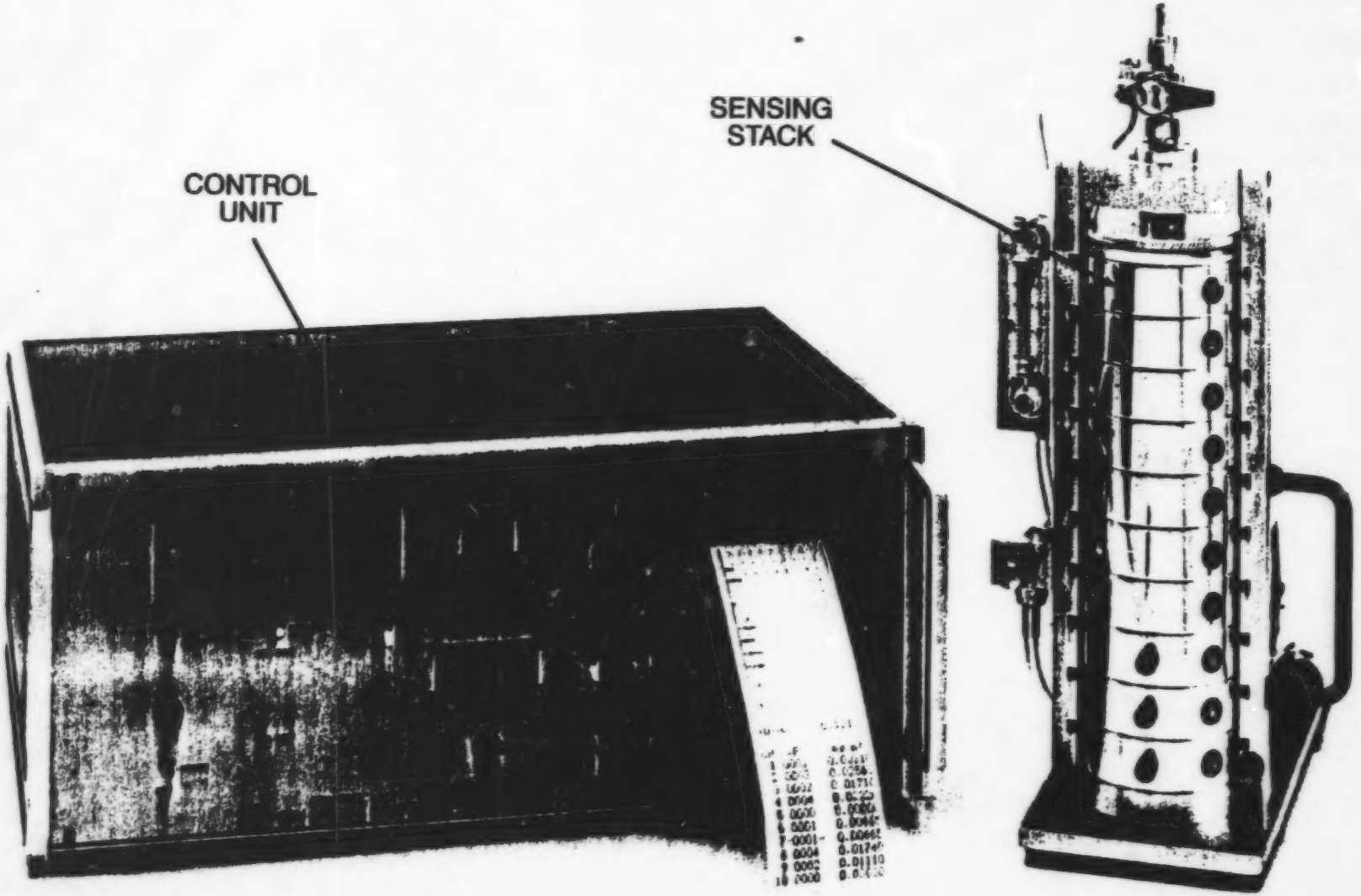

Fig. 20 - PC-2 aerosol analyzer.

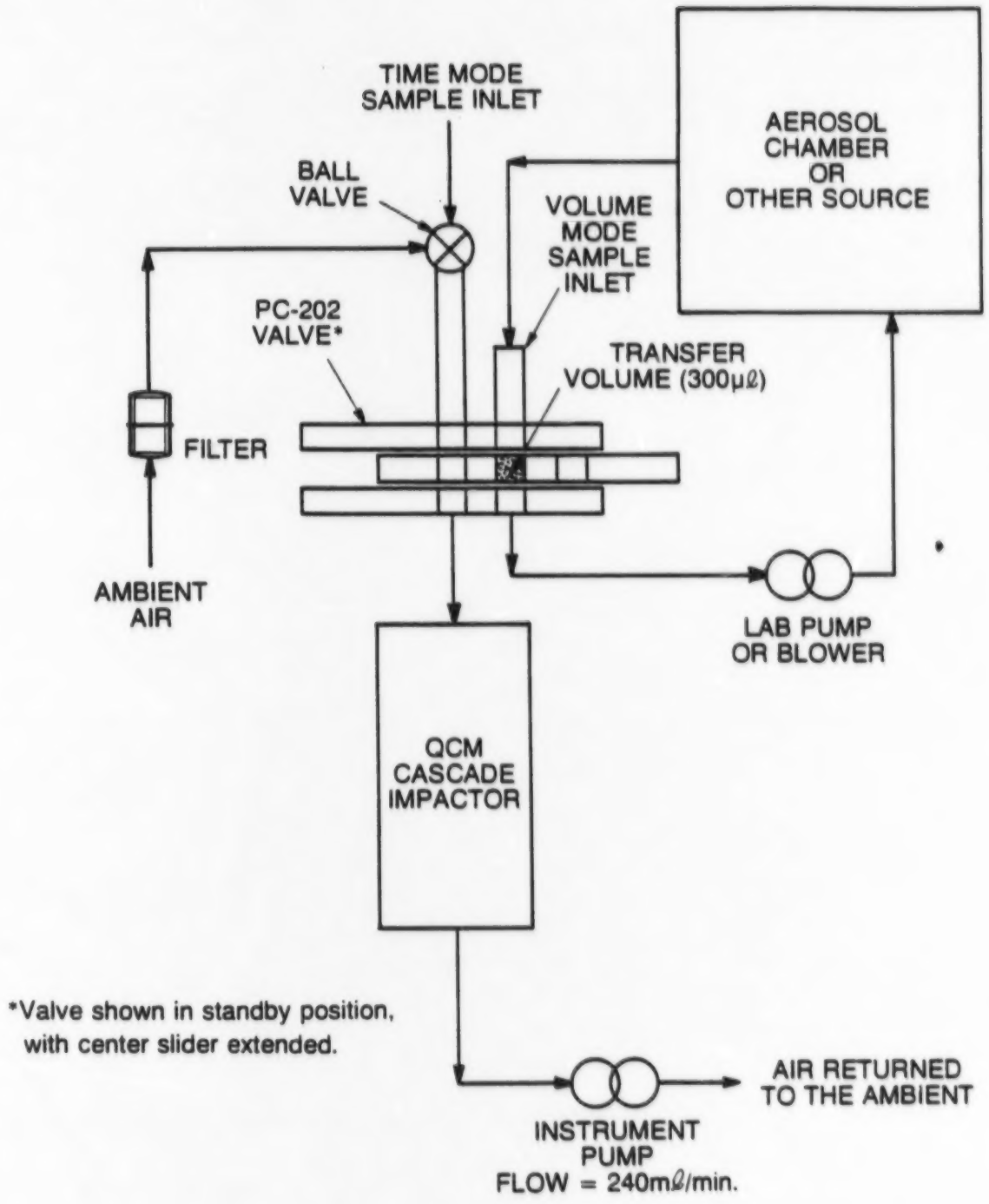

Fig. 21 - Flow diagram of PC-2 with PC-202 high concentration sliding valve.

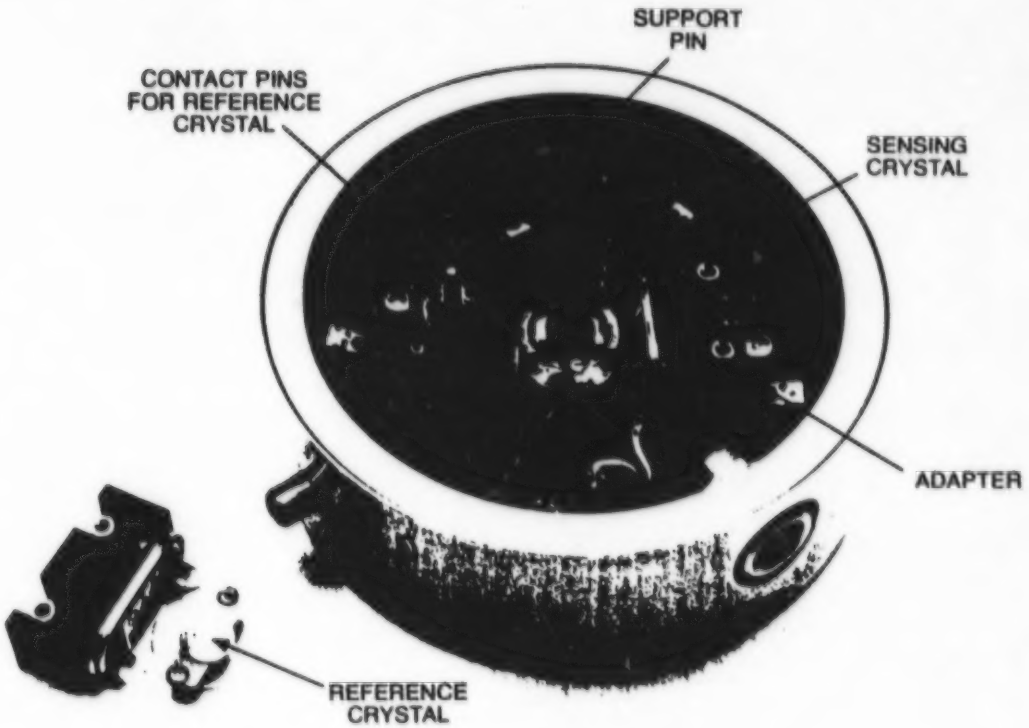

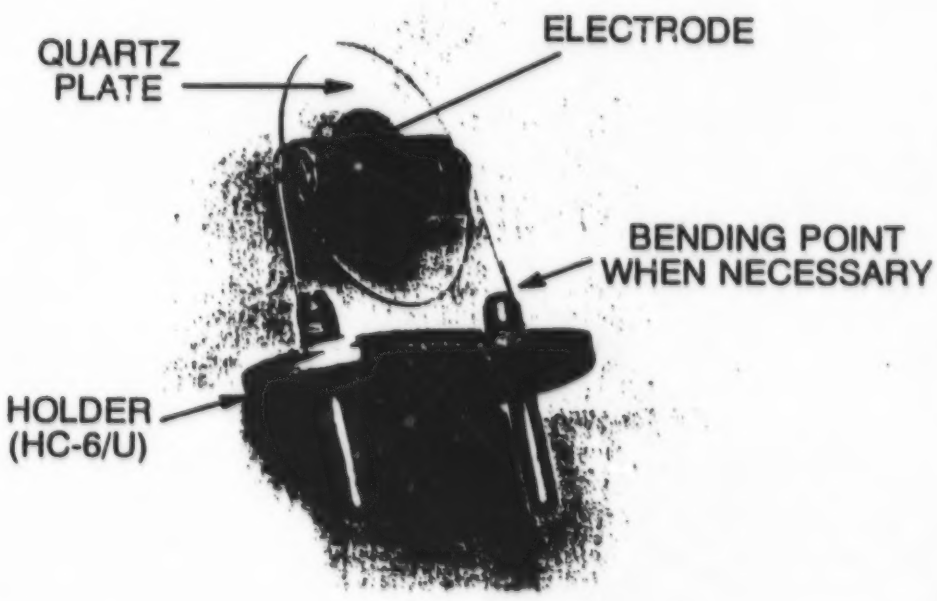

Fig. 22 - Details of the crystal assembly (upper drawing), and crystal (lower drawing).

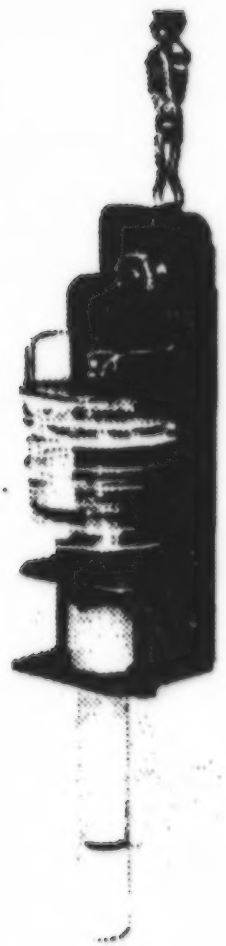

Fig. 23 - Nylon cyclone with filter holder and lapel bracket.

Fig. 24 - General view of an open-face dust sampler.

Fig. 25 - Views of the CEA track etch dosimeter (PAD).

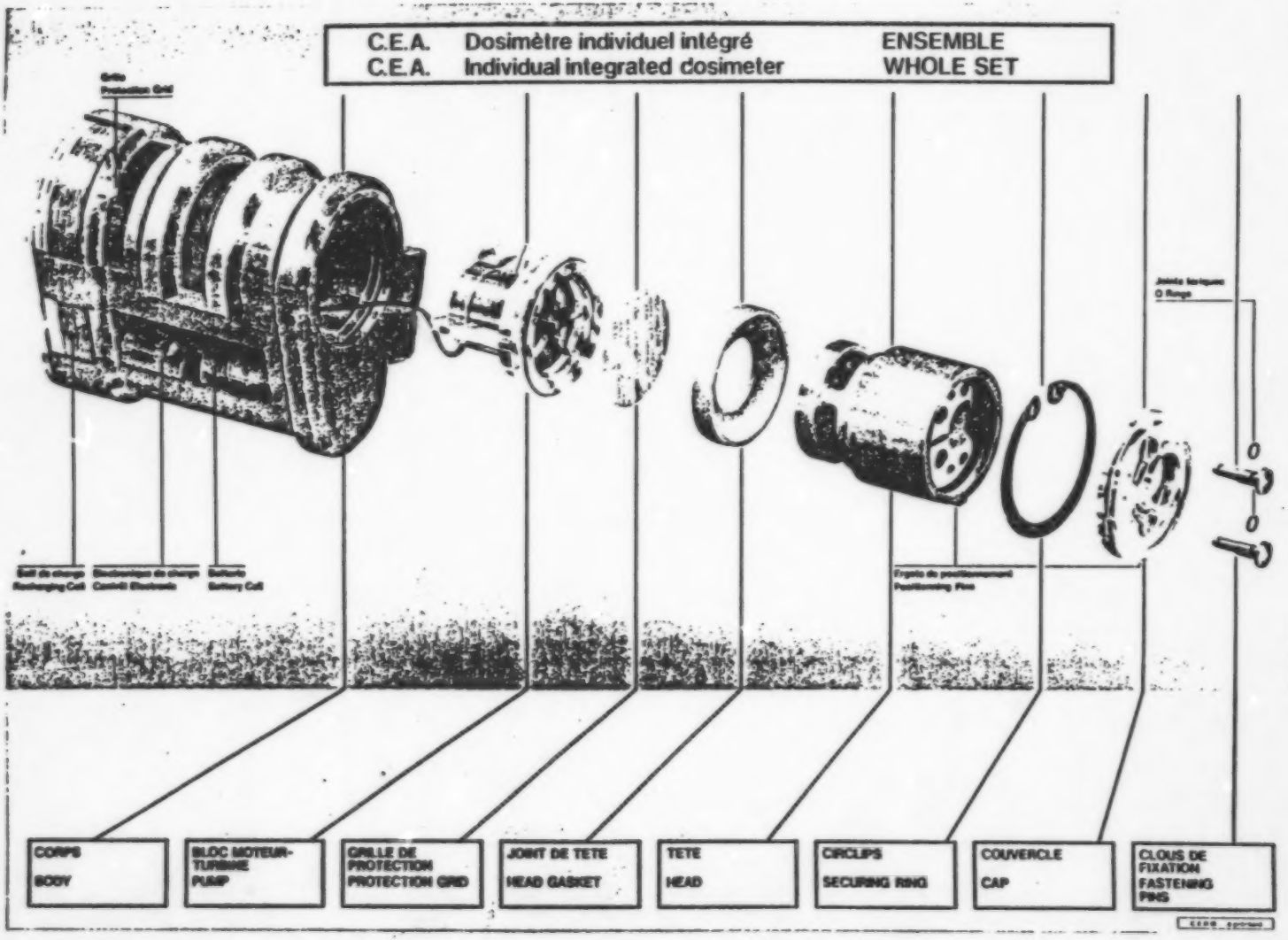

Fig. 26 - View of the CEA track etch dosimeter and components.

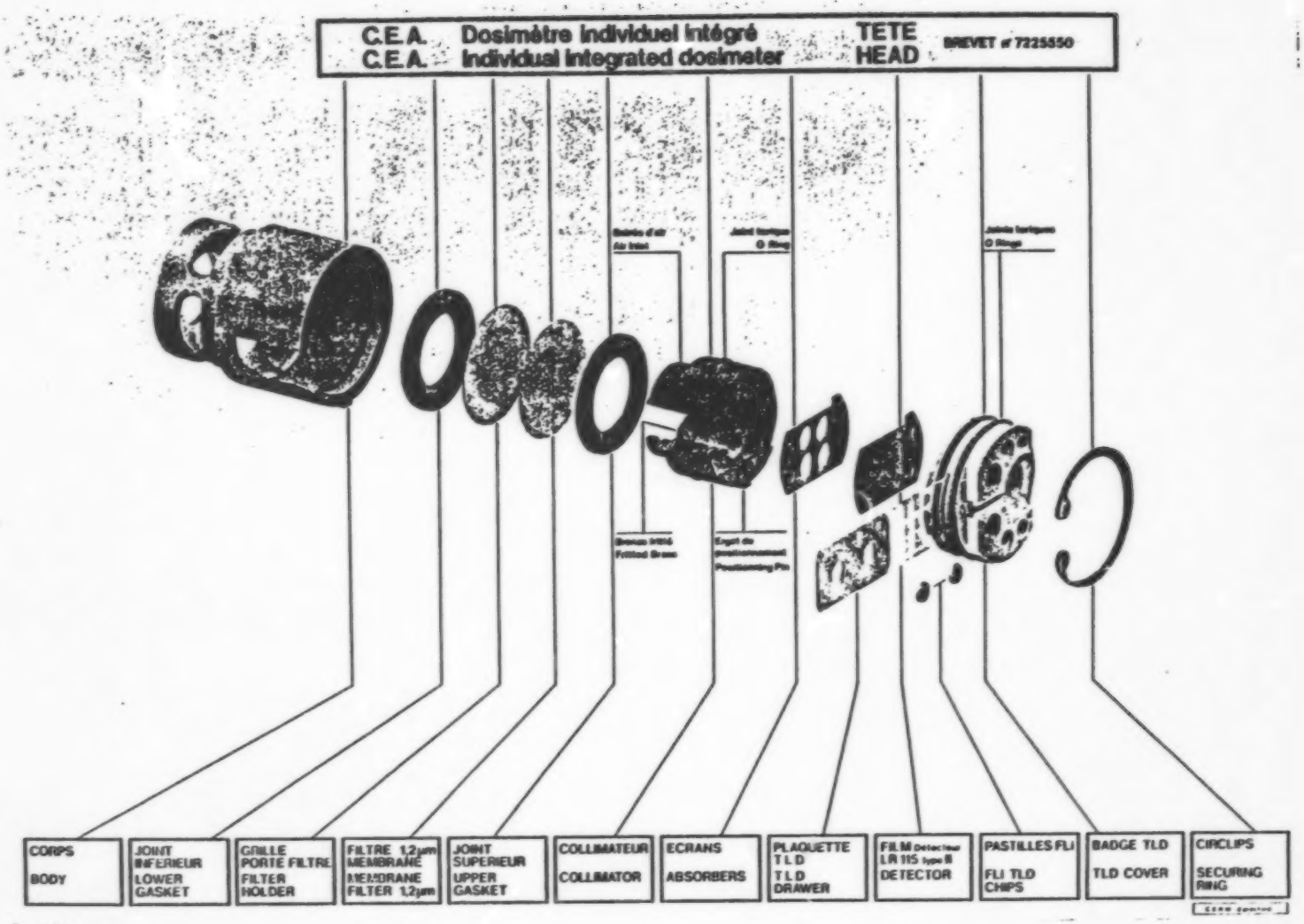

Fig.27 - Details of CEA track etch dosimeter sampling head.

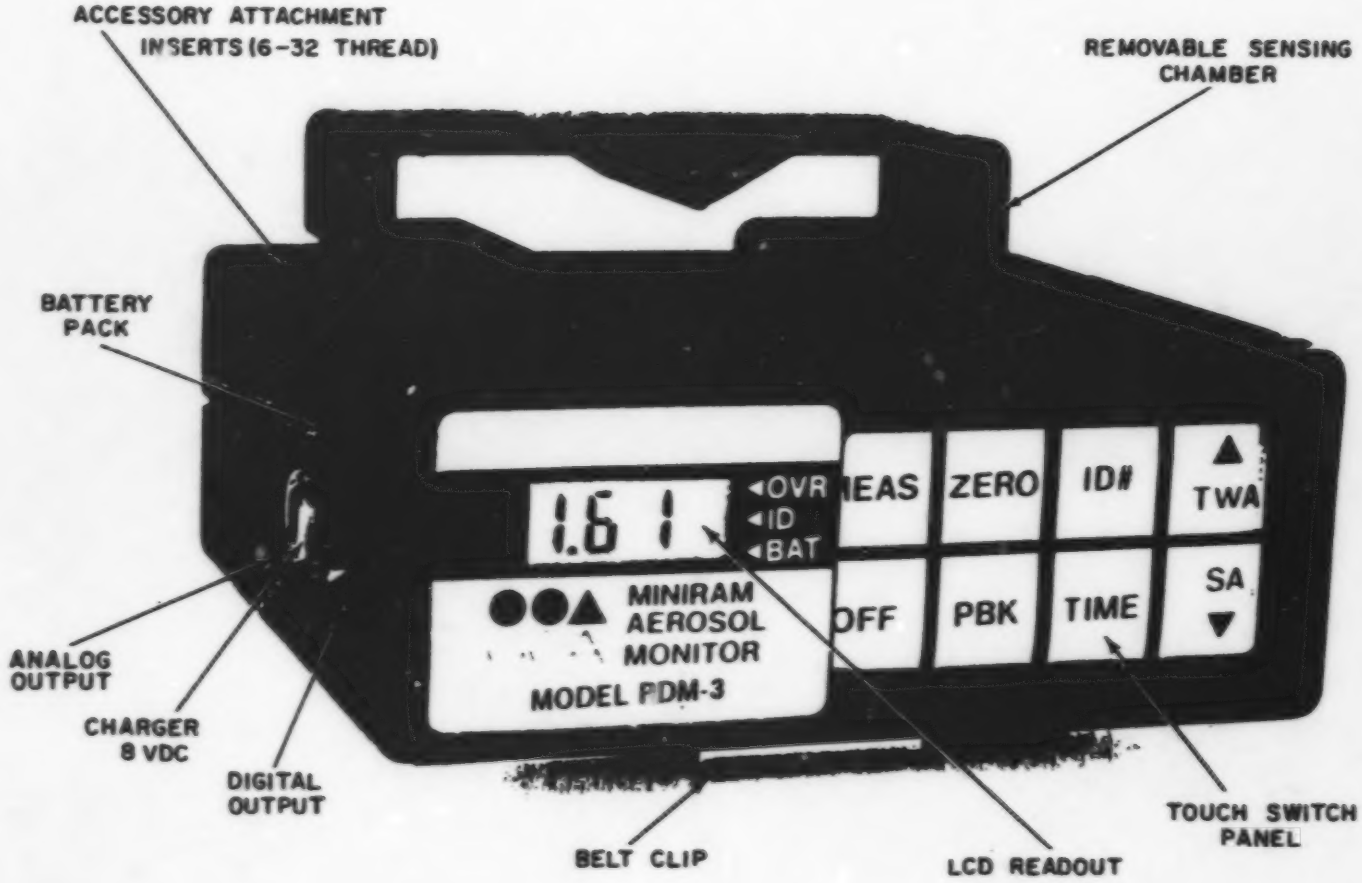

Fig. 28 - Main view of MiniRam.

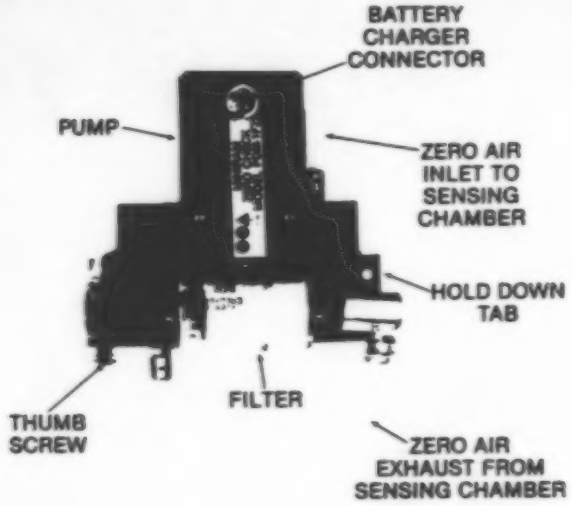

Fig. 29a - Zero Check Module

Fig. 29b - MINIRAM with Zero Check Module Attached

Fig. 29c - MINIRAM with Flow Adapter Attached

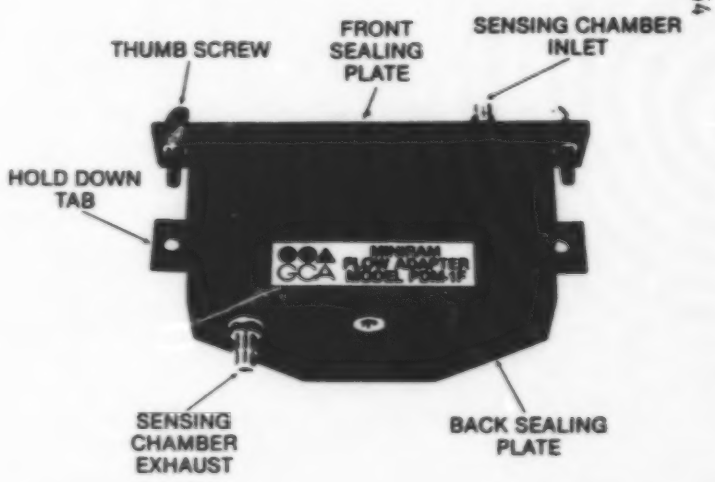

Fig. 29d - Flow Adapter

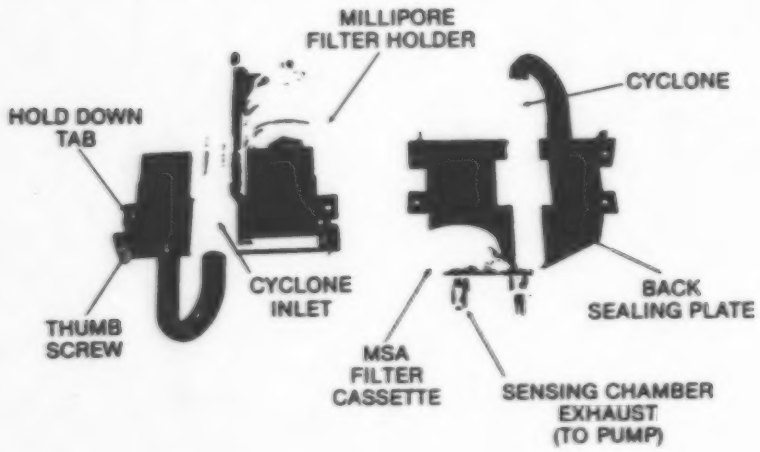

Fig. 30a - Personal Sampler Adapters

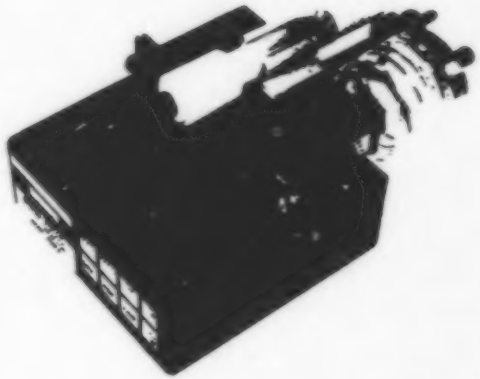

Fig. 30b - MINIRAM with Personal Sampler Adapter Attached

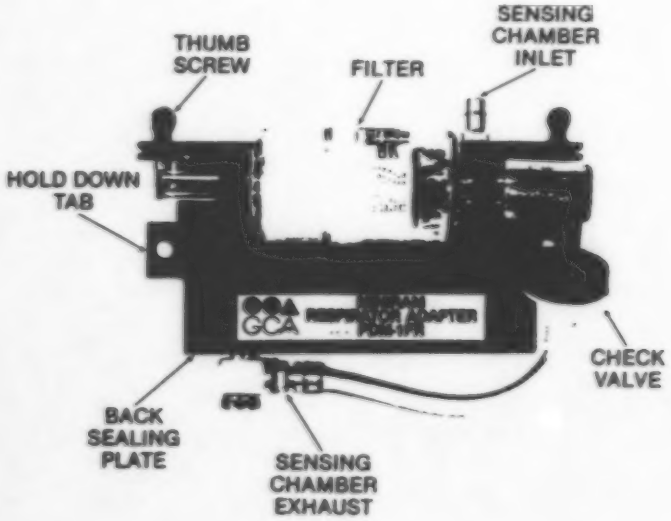

Fig. 30c - Respirator Adapter

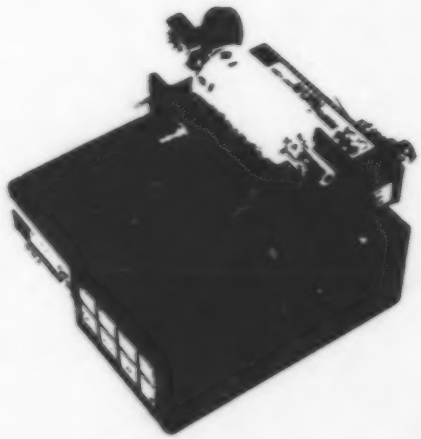

Fig. 30d - MINIRAM with Respirator Adapter Attached

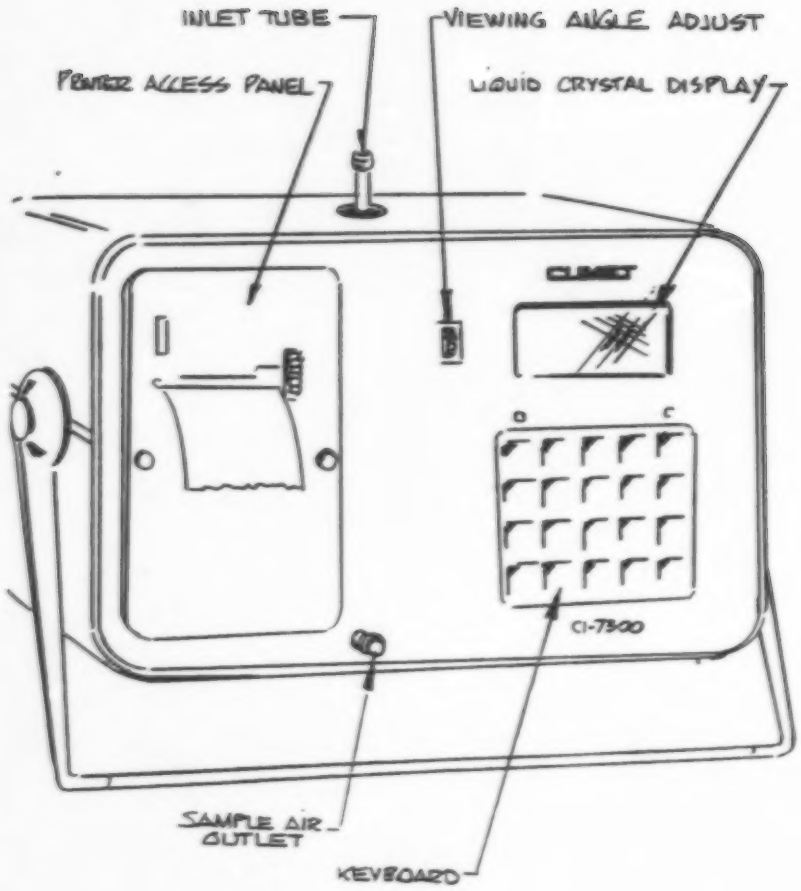

FRONT PANEL

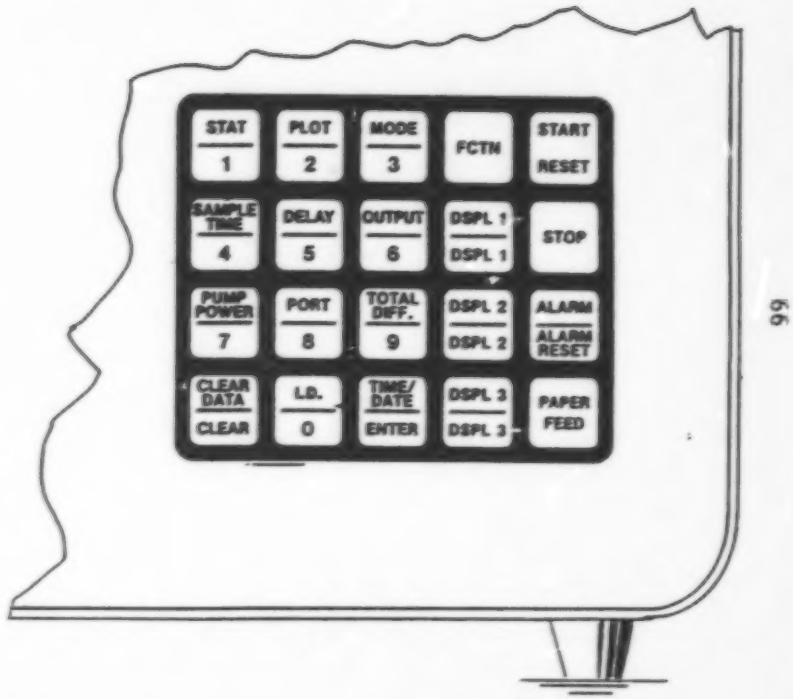

FRONT PANEL KEYPAD

Fig. 31 - Front view of the OPC CI-7300 (left hand side) and control panel of the same instrument (right hand side).

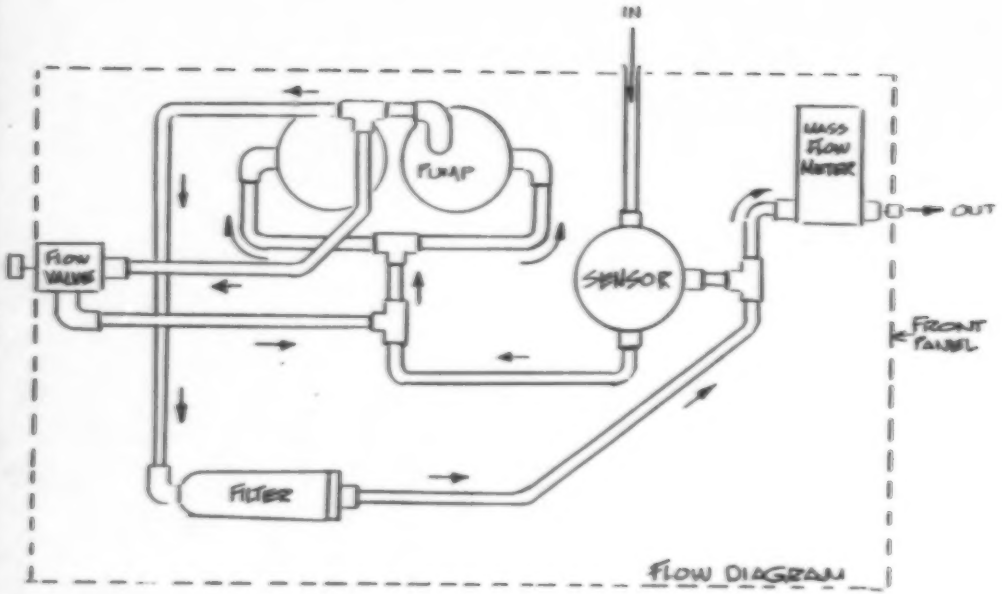

AIR SAMPLING SYSTEM

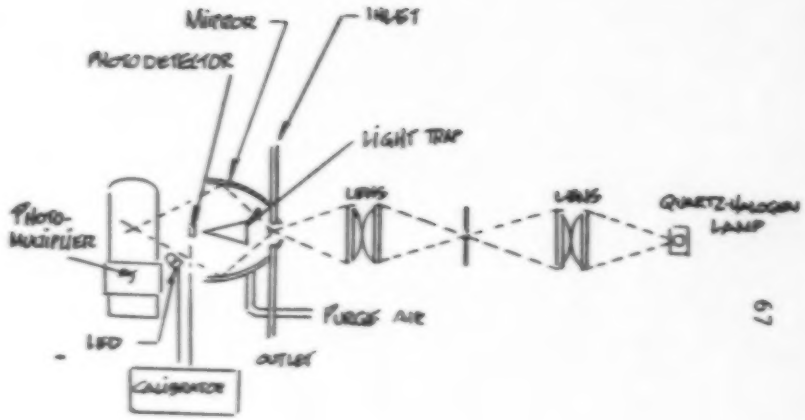

OPTICAL SYSTEM

Fig. 32 - Air sampling system (left hand side), and optical system (right hand side) of the OPC CI-7300.